Hybrid Encapsulated Ionic Liquids for Post-Combustion Carbon Dioxide (CO_2) Capture

Budget Period 2 - Topical Report

Reporting Period:	October 1, 2016 to September 30, 2017
Project Period:	October 1, 2015 to September 30, 2018
Principal Authors:	Joan F. Brennecke**, Thomas F. Degnan*, Mark J. McCready*+, Mark A. Stadtherr**, Joshuah K. Stolaroff***, and Congwang Ye***
	*University of Notre Dame, Department of Chemical and Biomolecular Engineering **University of Texas at Austin, McKetta Department of Chemical Engineering ***Lawrence Livermore National Laboratory +Principal Investigator
Date Report Issued:	November 1, 2017
DOE Award Number:	DE-FE0026465
Submitting Organization/: Recipient	University of Notre Dame du lac Office of Research 940 Grace Hall Notre Dame, IN 46556
Prepared for:	United States Department of Energy Office of Fossil Energy National Energy Technology Laboratory

DISCLAIMER

ABSTRACT

Ionic liquids (ILs) and Phase Change Ionic Liquids (PCILs) are excellent materials for selective removal of carbon dioxide from dilute post-combustion streams. However, they are typically characterized as having high viscosities, which impairs their effectiveness due to mass transfer limitations, caused by the high viscosities. In this project, we are examining the benefits of encapsulating ILs and PCILs in thin polymeric shells to produce particles of approximately 100 to 600 μm in diameter that can be used in a fluidized bed absorber. The particles are produced by microencapsulation of the ILs and PCILs in CO_2-permeable polymer shells. Here we report on the encapsulation of the IL and PCIL materials, thermodynamic testing of the encapsulated materials, mass transfer measurements in both a fluidized bed and a packed bed, determination of the effect of impurities (SO_2, NO_x and water) on the free and encapsulated IL and PCIL, recyclability of the CO_2 uptake, selection and synthesis of kg quantities of the IL and PCIL, identification of scale-up methods for encapsulation and production of a kg quantity of the PCIL, construction and shakedown of the laboratory scale unit to test the encapsulated particles for CO_2 capture ability and efficiency, use of our mass transfer model to predict mass transfer and identify optimal properties of the encapsulated particles, and initial testing of the encapsulated particles in the laboratory scale unit. We also show our attempts at developing shell materials that are resistant to water permeation.

Overall, we have shown that the selected IL and PCIL can be successfully encapsulated in polymer shells and the methods scaled up to production levels. The IL/PCIL and encapsulated IL/PCIL react irreversibly with SO_2 and NO_x so the CO_2 capture unit would need to be placed after the flue gas desulfurization and NO_x reduction units. However, the reaction with CO_2 in the presence of water is completely reversible. Therefore, it is not necessary to exclude water from the capsules. Mass transfer in the fluidized and packed beds confirm that the fluidized bed arrangement is preferred and that the mass transfer can be predicted accurately by the rate based model that we have developed. Absorption and desorption experiments in the laboratory scale unit show good uptake and recyclability.

TABLE OF CONTENTS

FIGURES IN THIS REPORT

FIGURES IN THIS REPORT

TABLES IN THIS REPORT

INTRODUCTION

The principal objective of this project is to demonstrate (TRL 3-4) the use of hybrid encapsulated ionic liquids (ILs) or phase change ionic liquids (PCILs) for post-combustion CO_2 capture. Encapsulated ILs/PCILs typically have high surface areas, allowing us to traverse the mass transfer barriers caused by high viscosities that are characteristic of ILs and PCILs.

This topical report describes work completed in Budget Period 2 of this project. The objectives for Budget Period 2 were to demonstrate scale-up of IL and/or PCILs encapsulation, show that the capsules retained high CO_2 capture efficiency and recyclability, determine the effect of impurities in the flue gas stream (including water) on the capsules and their CO_2 uptake, construct, test and use the laboratory scale unit, and use the rate-based model to guide capsule optimization.

RESULTS AND DISCUSSION

Budget Period 2 (BP2) was comprised of a single task for project management, two tasks that were carried over from Budget Period 1 (BP1) because of challenges encountered in the encapsulation of the IL and PCIL (Tasks 3 and 4) and nine technical tasks related to scale-up of the encapsulation, testing of encapsulated ILs and PCILs; use of the rate-based model to establish targets for necessary improvements in mass transfer; measurement of mass transfer coefficients, construction and shakedown of a laboratory-scale test unit and use of this unit for absorption and desorption tests (Tasks 7-16). The following describes work completed for the technical tasks.

Task 3.0 - Encapsulation of ILs

The ionic liquid (IL) and phase change ionic liquid (PCIL) chosen for use in this project are NDIL0230 (an IL) and NDIL0309 (a PCIL). In Budget Period 1 (BP1), we tested the uptake of NDIL0230 encapsulated in a particular polymer, SiTRIS, and found that it was lower than expected. The CO_2 uptake of samples of NDIL0230 encapsulated in SiTRIS received from LLNL on 5/12/16 and 7/7/16 met the criterion of having CO_2 uptake of at least 75% of the bulk values, as reported in the Topical Report on Year 1 and corresponding quarterly reports. However, detailed analytical work performed between 7/1/16 and 9/30/16 indicated that NDIL0230 was degrading and was not chemically compatible with SiTRIS. Even though NDIL0230 met the performance critera, we chose to be proactive in reducing long-term risk by seeking an alternative to SiTRIS. Therefore, work on Task 3 continued into BP2, focusing on Thiolene-Q as the shell material because detailed analytical work showed that NDIL0230 appeared to be compatible with Thiolene-Q. As described below, Thiolene-Q comprises a mixture of Thiolene with a liquid filler (commercial VQM-135 Q resin supplied by Gelest). LLNL efforts to encapsulate NDIL0230 and NDIL0309 in Thiolene-Q shells continued under Task 3 (specifically, Subtask 3.1 and 3.3) are described below.

During Budget Period 2 (BP2), we produced a suite of capsules with different shell materials and IL cores. We discovered chemical incompatibility and low gas permeability in a few sets of samples during characterization. We developed new shell material to overcome these issues. Batches of 1—25 g capsule samples were produced for CO_2 uptake and fluidization testing. The NDIL0230 formulation presented particular practical challenges, but those challenges have been overcome. After optimizing production setups and chemical formulations, both NDIL0230 and NDIL0309 have been successfully encapsulated with experimental performances that match theoretical prediction, and are thus considered successfully encapsulated.

Subtask 3.1 – Identification of IL and PCIL compatible shell materials and/or curing process

In the topical report on BP1, we reported the successful encapsulation of NDIL0231 in SiTRIS shell and NDIL0309 in Thiolene/silica (formerly called "Thiolene") shell. In BP2, we have successfully expanded the options and generated gram quantities of capsules with different shell materials containing the two chosen IL and PCIL, NDIL0230 and NDIL0309, and some examples are shown in **Figure 1**.

We were able to further refine the fabrication conditions to reproduce these capsules with faster shell curing and thinner capsule walls. We were also able to explore heated encapsulation of higher purity IL. We designed and assembled a heating stage (**Figure** 2, top left) that would allow high temperature drop generation. Although neat NDIL0230 would be chemically compatible with Thiolene-Q and could be potentially encapsulated with the neat solvent when loaded, we were unable to flow them in microfluidic devices for stable drop generation due to their high viscosities at room temperature. Since their viscosities drop about one order of magnitude when heated to 70 °C **(Figure 2,** lower left), we projected that we could use the heating stage to potentially achieve neat solvent encapsulation.

As shown in **Figure 2**, when temperature increases during drop generation, the co-axial fluid jet of core-shell gradually shifted from jetting to dripping, producing more monodisperse drops. We should note that the shell thickness was not ideal in this case because the extremely low viscosity SiTRIS shell phase was used in this trial. Shell thickness can be lowered when we switch to the silicones. At the same time, we also retrofitted the setup so that it can provide enough energy to heat up the device to the desired temperature.

While heating reduces the fluid viscosities (improving encapsulation conditions), we also noticed a sharp reduction in interfacial tension between core and shell fluids, preventing good capsule formation. Despite these difficulties, some Thiolene-Q capsules with neat NDIL0230 core were successfully produced. Our work on the heating stage was discontinued to focus on long-term continuous production of NDIL0230-Thiolene-Q capsules at room temperature for faster turn-around on sample production and an easier path to scale-up.

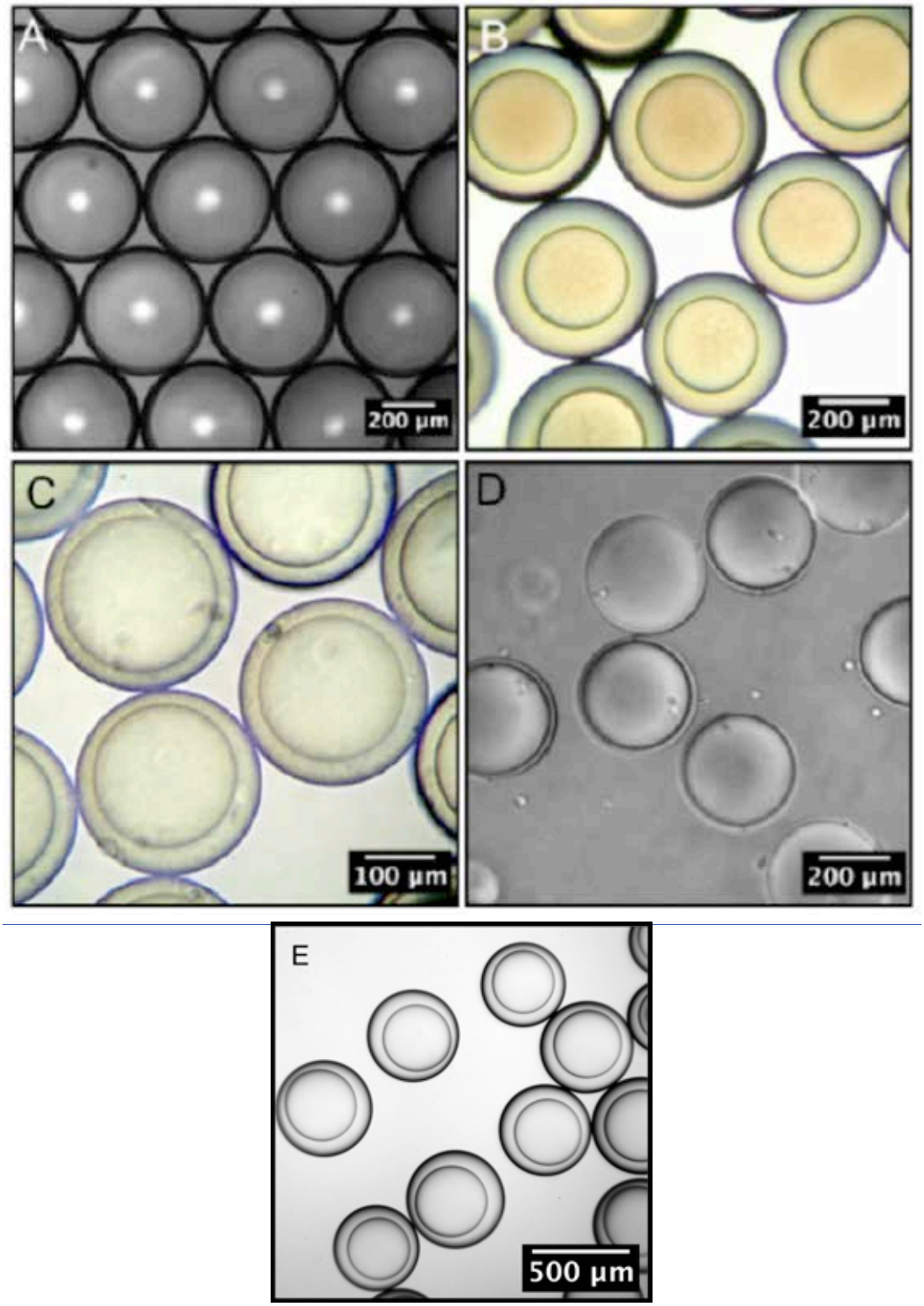

Figure 1: Images of IL Microcapsules produced in the course of this project.
A: NDIL0231 / Water-SiTRIS; **B:** NDIL0230 / Water-SiTRIS; **C:** NDIL0309 / Water-Thiolene-Q/Silica**; D:** NDIL0309 / Water-Thiolene-Q; **E:** NDIL0230 / Water-Thiolene-Q

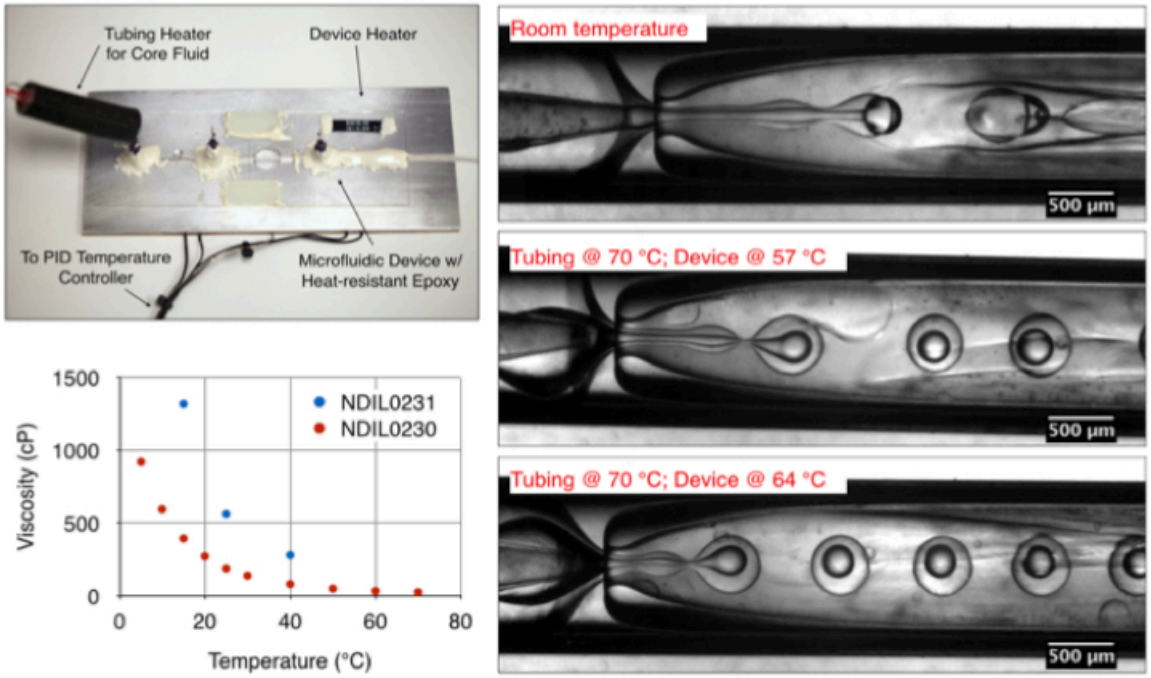

Figure 2: Viscosity change of NDIL0230 and NDIL0231 as a function of temperature. Also shown is the change in drop generation from "jetting" to "dripping" as temperature increases. These images were generated using the external heating stage.

In the previous Budget Period (BP1), we produced the Thiolene shell material with a fumed silica filler. In Budget Period 2, we noted that the fumed silica degrades over time during storage, resulting in large quantities of aggregated silica in the mixture. This aggregation causes instability in fluid flow, and often leads to clogging in the device (see Figure 3). However, we cannot simply remove fumed silica, as it is needed to improve the mechanical properties. To resolve this issue, we reformulated Thiolene with a liquid filler (VQM-135 Q resin from Gelest) that produced a more homogeneous mixture while also maintaining good mechanical strength; resulting in a material we termed Thiolene-Q.

The initial mixture of Thiolene-Q was too viscous to efficiently flow in microfluidic devices, but reducing the filler fraction solved this problem. The resulting Thiolene-Q mixture was used to encapsulate NDIL0309 and NDIL0230, and successfully produced capsules with a thinner shell and better stability, as shown above.

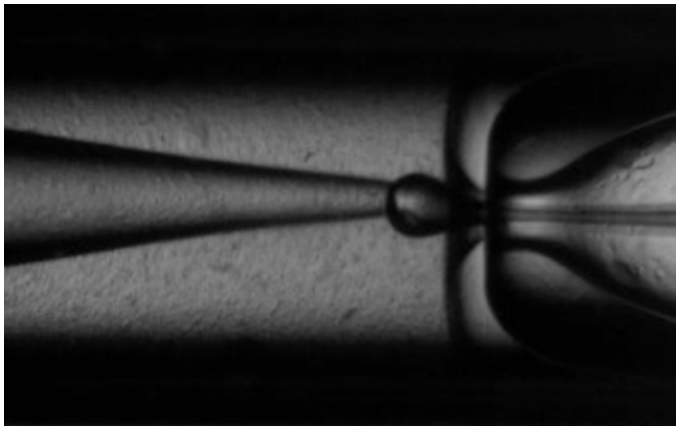

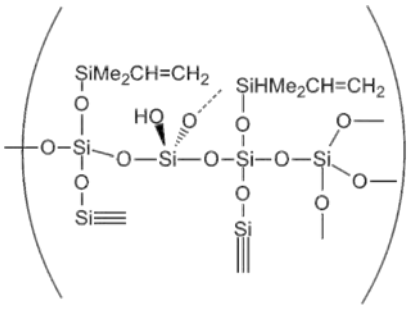

Figure 3: Left: Aggregated silica, seen as impurity in the original Thiolene-Q / Silica mixture; Right: Structure of Q-Resin which was used to produce the new Thiolene-Q that has resolved the "clogging issue."

This success, taken with results of the chemical compatibility studies and the reprotonation analysis, led us to select Thiolene-Q as the preferred shell material for both NDIL0230 and NDIL0309.

Subtask 3.2 – First production of small quantities of encapsulated ILs

This subtask was completed in Budget Period 1.

Subtask 3.3 – Production of a suite of small quantities of encapsulated ILs

During BP2, LLNL produced a suite of small samples of both encapsulated NDIL0309 and encapsulated NDIL0230. As described in Task 4.0 below, Thiolene-Q encapsulated NDIL0309 and NDIL0230 particles have been produced that meet CO_2 uptake criteria.

Table 1 shows a list of the capsules and materials produced at LLNL and sent to Notre Dame for material characterizations and fluidization tests during BP2.

Many challenges were encountered, especially in the encapsulation of NDIL0230. A number of the NDIL0230 capsule samples displayed CO_2 capture capacity 10-20% less than expected value, and we proposed that it was because of the small ratio of broken/empty capsules from the production (see **Figure 4a**). The root cause of this is the lack of interface stability between core and shell. While developing polymer formulation for another scale-up production apparatus, LLNL discovered that different shell polymer photoinitiators affect the interfacial tension and interface stability. After a systematic screening of the different formulations, Thiolene-Q with a new photoinitiator, TPO-L, was selected as the most promising candidate in production. Stable capsule production was thus achieved (see **Figure 4b**). The core fluid is composed of 50% NDIL0230, 2.5% glycerol, 1% Poly vinyl alcohol and water and the IL% in the final dry sample was 40% (see **Figure 4c**). Additionally, we discovered that the IL mixture, while stored in plastic

syringe for weeks, would cause instability in drop generation so fresh mixtures have been used to achieve consistent production.

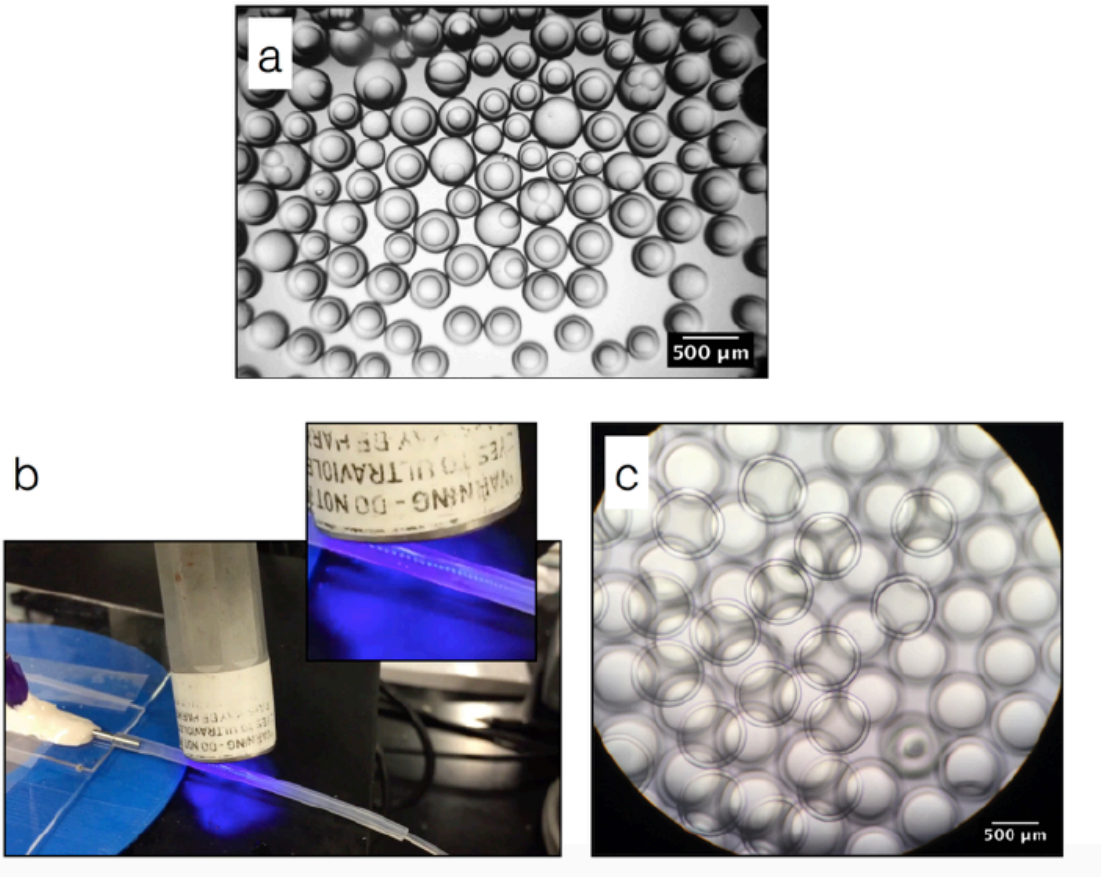

Figure 4: Images of a) NDIL0230-Thiolene-Q capsules produced at LLNL with size variation, b) stable production of NDIL0230-Thiolene- Q (TPO-L) capsules, and c) as-produced NDIL0230-Thiolene-Q (TPO-L) capsules. All samples were produced with a core fluid of 50% NDIL0230, and then dried to remove water.

Production of both small batch and larger quantities of NDIL0309 (70% in water) encapsulated in Thiolene-Q occurred through most of BP2, as detailed in **Table 1.**

Table 1: List of samples that have been shipped from LLNL to Notre Dame for testing.

Date Rec'd	Amount	Samples	Notes
10/18/16	3 g	NDIL0309 in Thiolene-Q capsules	Capsules were saturated with CO2 during LLNL tests
	1 piece	Thiolene-Q membrane	
	5 g	Thiolene-Q resin	
	3 g	3% sodium carbonate in TR2650 capsules	
10/21/16	5 g	Thiolene-Q resin (correct ratio)	
11/11/16	30 g	17% sodium carbonate in TR2650 capsules	Dusted with silica powder
11/17/16	1 g	Thiolene-Q capsule with empty core	
12/2/16	10 g	NDIL0309 in Thiolene-Q capsules	5 vials made on different days, each with specific flow rates
12/20/16	30 g	NDIL0309 in Thiolene-Q capsules	8 vials made on different days, each with specific flow rates
	1 g	Silica powder	
4/4/17	5 g	NDIL0230 in Thiolene-Q capsules	a preliminary run with high% of empty capsules
5/18/17	29 g	NDIL0309 in Thiolene-Q capsules	
6/6/17	1 g	NDIL0230 capsules-old	capsules left in glycerol solution for 2 weeks
	4 g	NDIL0230 capsules-fresh	capsules with lower empty%
7/31/17	6 g	Dry NDIL0230 in Thiolene-Q capsules	Capsules with empty % characterized
8/4/17	4 g	Dry NDIL0230 in Thiolene-Q (TPO-L) capsules	Capsules have high core % of 30-40%
9/13/17	300 g	Dry NDIL0309 in Thiolene-Q capsules	From Dolomite setup
9/21/17	5 g	Dry NDIL0230 in Thiolene-Q (TPO-L) capsules	Capsules have high core % of 30-40%
9/28/17	300 g	Dry NDIL0309 in Thiolene-Q capsules	From Dolomite setup
10/6/17	300 g	Dry NDIL0309 in Thiolene-Q capsules	From Dolomite setup
	3 g	Thiolene-Q (TPO-L) cured and uncured shell materials	For shell material study

Task 4.0 - Testing of Encapsulated IL Particles

Subtask 4.1 - Thermodynamic testing

Due to continuing work by LLNL in BP2 on encapsulation of NDIL0230 and NDIL0309 (Task 3), we continued work in BP2 on the testing of the small samples of encapsulated IL particles. The thermodynamic testing of encapsulated NDIL0309 was completed by 6/30/17 and was completed for encapsulated NDIL0230 by 9/30/17.

The first capsules of the PCIL (NDIL0309) were received from LLNL on 5/12/16 and they were encapsulated using Thiolene-Q as the shell material.. The water content of the PCIL used during encapsulation was unknown so the PCIL content had to be estimated from analytical tests after the CO_2 uptake was performed. Based on this analysis, these capsules met the criterion of >75% capacity compared to the free PCIL material, as reported in the Topical Report on BP1 and corresponding quarterly reports.

Below we report on thermodynamic testing done in BP2 on samples of NDIL0309 encapsulated in Thiolene-Q. This is followed by recent work on NDIL0230 encapsulated in Thiolene-Q.

NDIL0309 encapsulated in Thiolene-Q

The next sample (after 5/12/16) of encapsulated PCIL (now in the Thiolene polymer with a filler – Thiolene-Q) was received 10/18/16. First, we measured the physical uptake of CO_2 in the Thiolene-Q shell material and those data are shown in **Figure 5.** These measurements were performed in the Hiden Intelligent Gravimetric Microbalance.

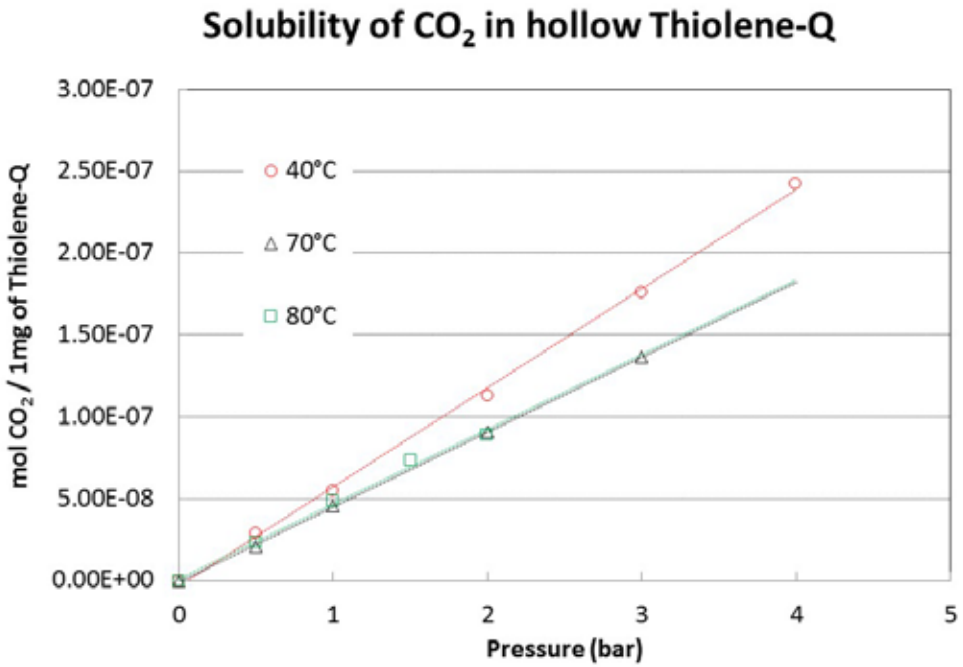

Figure 5: Solubility of CO_2 in the Thiolene-Q polymer shell material.

We then measured the CO_2 uptake by the NDIL0309 encapsulated in Thiolene-Q (sample received 10/18/16). When the physical solubility of the CO_2 in the shell material is subtracted from the total uptake, the uptake for the encapsulated NDIL0309, based on the flow rates of core material and shell material in the LLNL microfluidic device, compares favorably with the uptake for the pure material, as shown in **Figure 6**. There was some uncertainty in the weight% of NDIL0309 in these capsules because LLNL did not know the amount of water in the NDIL0309 when they prepared the aqueous solution for the core of the capsules. This motivated our preparation of stock solutions of NDIL0309 in water for LLNL to use in the microfluidic device. A composition of 25 wt% was assumed for this sample to calculate the values in **Figure 6**.

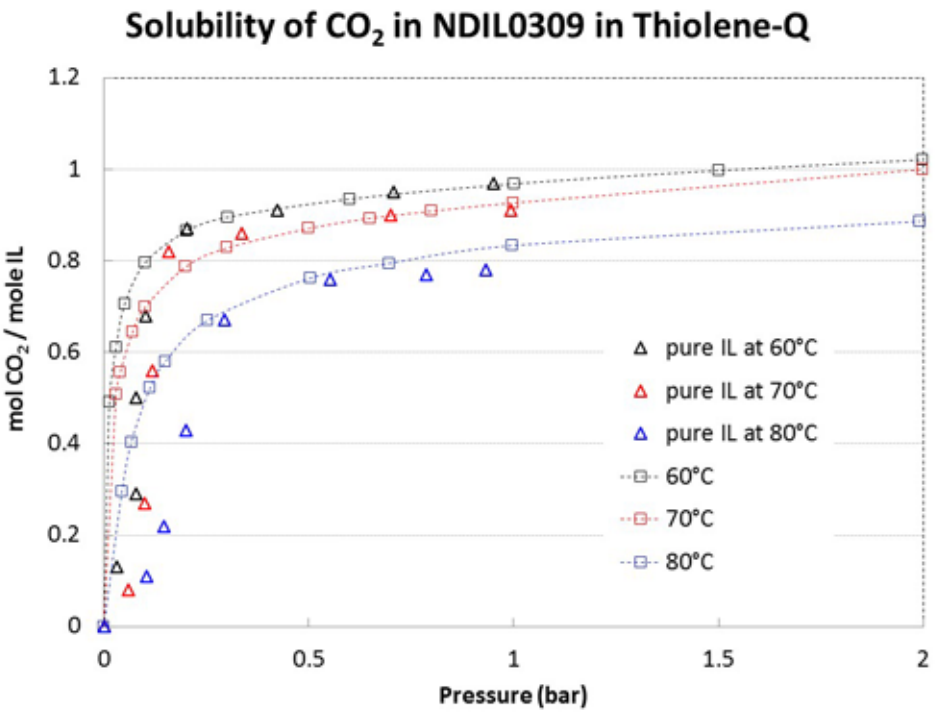

Figure 6: Equilibrium solubility of CO_2 in Thiolene-Q encapsulated NDIL0309 (received Oct. 19, 2016). For these measurements the capsules had been evacuated to remove all water. The uptake has been corrected for physical dissolution in the polymer shell material (**Figure 5**).

We then attempted to cycle the CO_2 uptake of the Thiolene-Q encapsulated NDIL0309 (received 10/18/2016). The goal with this sample was to show cycling of the CO_2 uptake. The uptake experiments were performed at 80 °C, with desorption at 90 °C until the sample returned to its original mass. Unfortunately, the uptake values for the second and third cycles did not match the first cycle (they were actually increasing). This is shown in **Figure 7**. Therefore, we removed the sample from the gravimetric microbalance. We noted that the capsules had turned brown in color. We broke the shells open and performed ^{1}H NMR analysis, which showed that the anion peaks were reduced in intensity compared to the cation peaks by approximately 50%. As a control, we broke open some of the as-received capsules and performed ^{1}H NMR analysis. The PCIL inside those capsules was as expected, unchanged,, maintaining a 1:1 anion to cation ratio.

We also analyzed a sample that had been subjected to one absorption and desorption cycle. The material from inside those capsules had also decomposed, with anion peaks reduced in intensity compared to the cation peaks by approximately 50%. This result was surprising since we had tested the compatibility between the Thiolene-Q and the ILs and PCILs (reported in the Topical Report for BP1) and saw no decomposition or degradation of either the IL/PCIL or polymer. However, we noteed that the compatibility tests were performed at room temperature, while drying, CO_2 absorption and desorption in the

gravimetric microbalance was done at temperatures between 60 and 90 °C. In addition, there was no CO_2 present in the Thiolene-Q + IL/PCIL compatibility tests. The 10/18/16 capsules met the uptake criterion. However, uptake cycling tests indicated an increase in the CO_2 uptake with some possible degradation of the PCIL, as determined by ^{1}H NMR. We were not able to repeat these tests in 2016 due to a lack of sufficient samples. Fortunately, we did not jump to any conclusions about incompatibility between Thiolene-Q and the PCIL. Subsequent tests with samples of NDIL0309 encapsulated in Thiolene-Q (samples received 12/2/16 and 12/20/16) showed that they are compatible and can be recycled. See below.

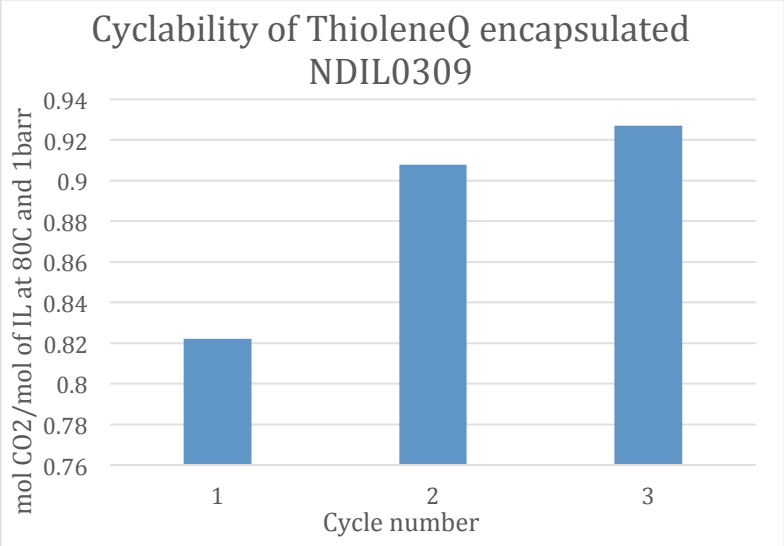

Figure 7: CO_2 uptake at 80 °C and 1 bar for three cycles of Thiolene-Q encapsulated NDIL0309 (sample received Oct. 18, 2016). For these measurements the capsules had been evacuated to remove all water. The uptake has been corrected for physical dissolution in the polymer shell material (**Figure 5**).

As reported above, we received several small samples of NDIL0309 encapsulated in Thiolene-Q during December 2016 (see **Table 1**). Subsequently, we tested these samples. We measured the CO_2 uptake of four different batches of the NDIL0309 in Thiolene-Q at 80°C in the Hiden Gravimetric Microbalance. The samples are evacuated under vacuum at 90°C until a constant mass was obtained. Then absorption was performed at pressures up to 1 bar. As shown in **Figure 8**, the uptake by the difference batches is identical within experimental uncertainty. Moreover, the uptake values match those determined for the free PCIL material, also within experimental uncertainty. The weight percent of active PCIL material in the dried capsules was calculated from the flow rates of PCIL solution and polymer solution used in the microfluidic device. This demonstrates excellent performance and superb reproducibility.

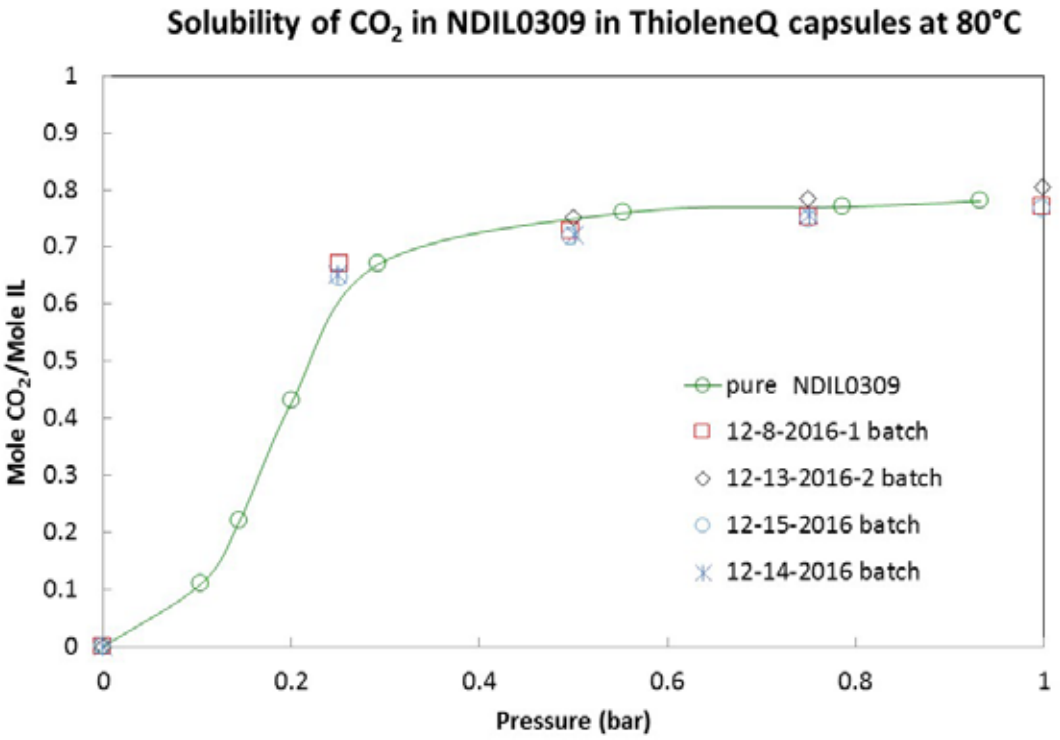

Figure 8: Solubility of CO_2 in various batches of NDIL0309 encapsulated in Thiolene-Q at 80 °C. For these measurements the capsules had been evacuated to remove all water. The uptake has been corrected for physical dissolution in the polymer shell material (**Figure 5**). Batch numbers correspond to dates that the samples were produced by LLNL. These samples were received on 12/20/2016.

We have also performed recyclability testing of the NDIL0309/Thiolene-Q capsules. For this test we used one of the batches produced on December 8, 2016 (received 12/20/2016). These experiments were also performed in the Hiden Gravimetric Microbalance. Following each absorption cycle, the system was evacuated under vacuum at 90°C until the mass leveled out and returned to the original value. Then the next absorption cycle was performed. As shown in **Figure 9**, there is absolutely no degradation in performance even after four absorption and desorption cycles. This was confirmed by ^{1}H NMR analysis.

From these experiments we have concluded that NDIL0309 encapsulated in Thiolene-Q is chemically stable, recyclable, and reproducible. We have demonstrated that Thiolene-Q is compatible with NDIL0309.

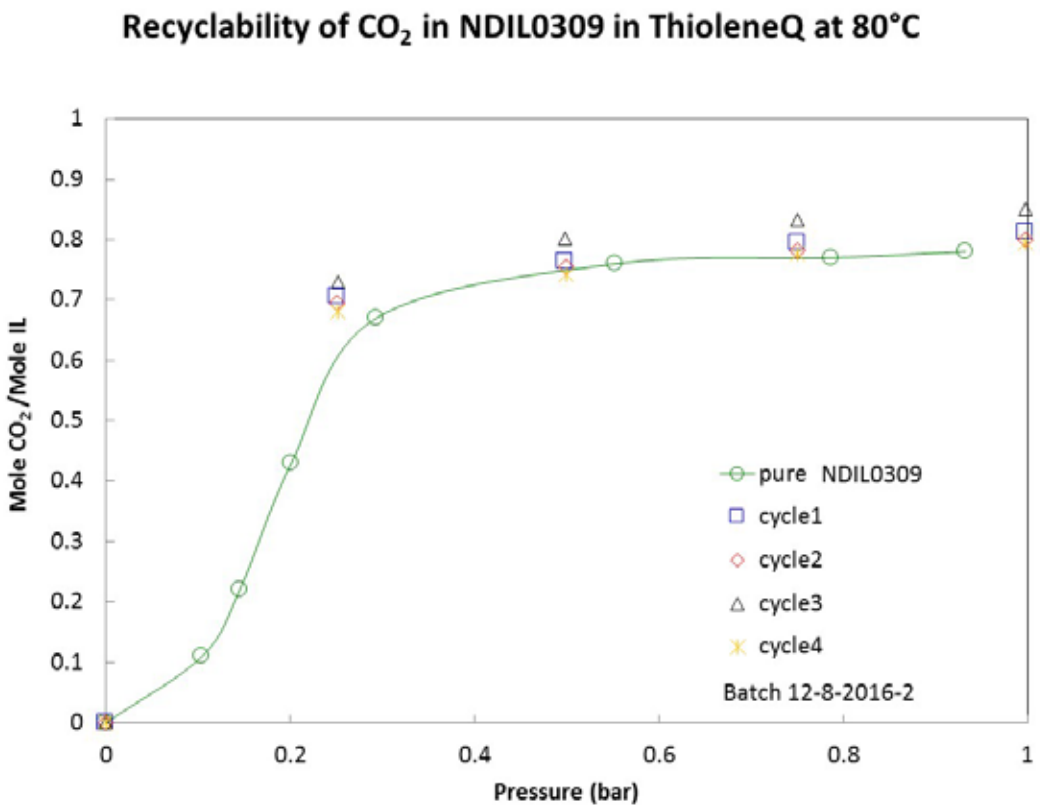

Figure 9: Recyclability of the CO_2 uptake in NDIL0309 encapsulated in Thiolene-Q at 80 °C. For these measurements the capsules had been evacuated to remove all water. The uptake has been corrected for physical dissolution in the polymer shell material (**Figure 5**).

NDIL0230 encapsulated in Thiolene-Q

As reported above in Subtasks 3.1 and 3.3, encapsulation of the IL (NDIL0230) in Thiolene-Q was quite challenging. The first samples were received in April, 2017 (see **Table 1**). CO_2 uptake results at 20 °C for two samples of these capsules are shown in **Figures 10** and **11**. These samples are two vials from the same production day (3/21/17; received 4/4/17) and they show the same results. The uptakes are roughly half what would be expected based on the flow rates used in the microfluidic device. Moreover, ^{1}H NMR analysis of the capsule contents from vial 4 both before and after CO_2 capture show some anion degradation.

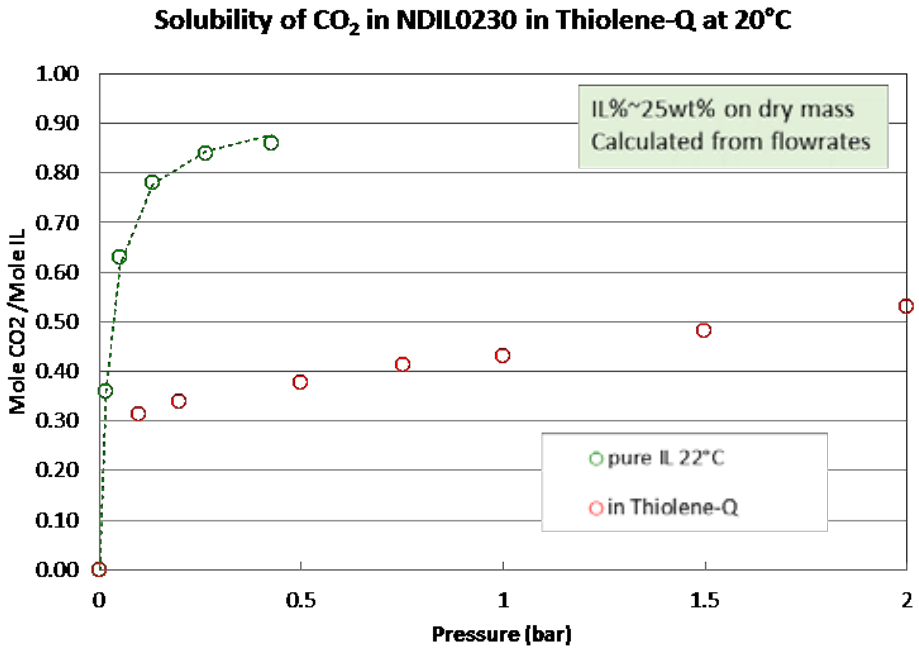

Figure 10: Solubility of CO_2 in NDIL0230 encapsulated in Thiolene-Q at 20 °C (vial 4 of batch produced on 3/21/17). For these measurements the capsules had been evacuated to remove all water. The uptake has been corrected for physical dissolution in the polymer shell material (**Figure 5**).

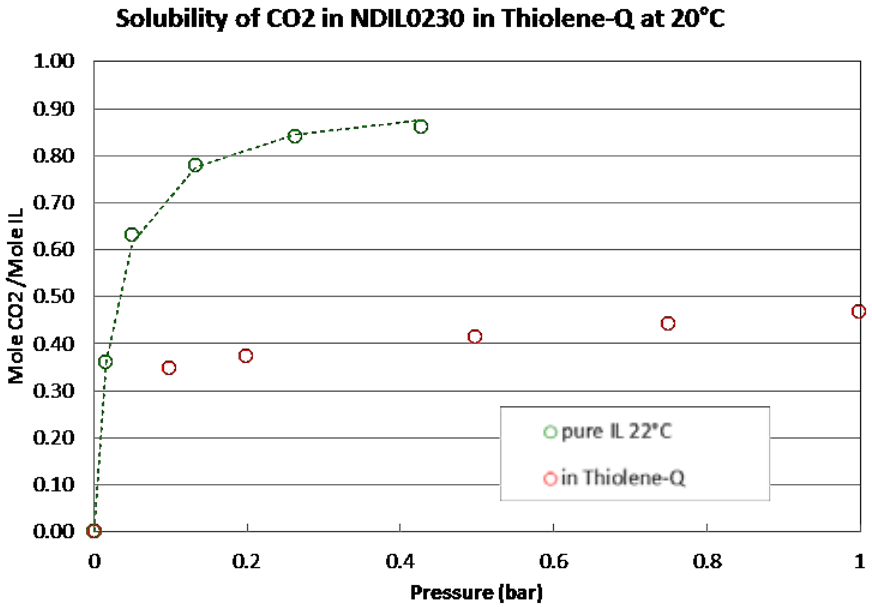

Figure 11: Solubility of CO_2 in NDIL0230 encapsulated in Thiolene-Q at 20 C (vial 3 of batch produced on 3/21/17). For these measurements the capsules had been evacuated to remove all water. The uptake has been corrected for physical dissolution in the polymer shell material (**Figure 5**).

The next samples of NDIL0230 encapsulated in Thiolene-Q were received in June, 2017 (see **Table 1**). The CO_2 uptake for these two samples is shown in **Figures 12** and **13**. Based on the flow rates in the microfluidic device the IL content of the dried capsules should be 18 wt% for the sample produced on 5/16/17. Based on this number, the CO_2 uptake is about 25% lower than expected. Moreover, the ^1H NMR of the 5/16/17 sample showed degradation of the IL both as received and after CO_2 uptake. Conversations with LLNL suggested two possible explanations: exposure to much higher UV radiation during curing of the polymer shell or soaking of the capsules in the production fluid for about two weeks before the capsules were recovered and dried. The CO_2 uptake for the sample produced on 5/30/17 was within about 15% of the expected uptake based on the flow rates used in the microfluidic device. This is a significant improvement over samples received and tested in April and the relatively small discrepancy might be attributed to some percentage of empty shells. The ^1H NMR analysis of the core material for the 5/30/17 sample showed that the IL was fine both before and after CO_2 uptake and there was no evidence of degradation.

Based on these tests, NDIL0230 appeared to be compatible with Thiolene-Q. We demonstrated that the IL can be successfully encapsulated using this polymer system. However, the IL content of the dried capsules for both of these samples was quite low and not sufficient for the intended application.

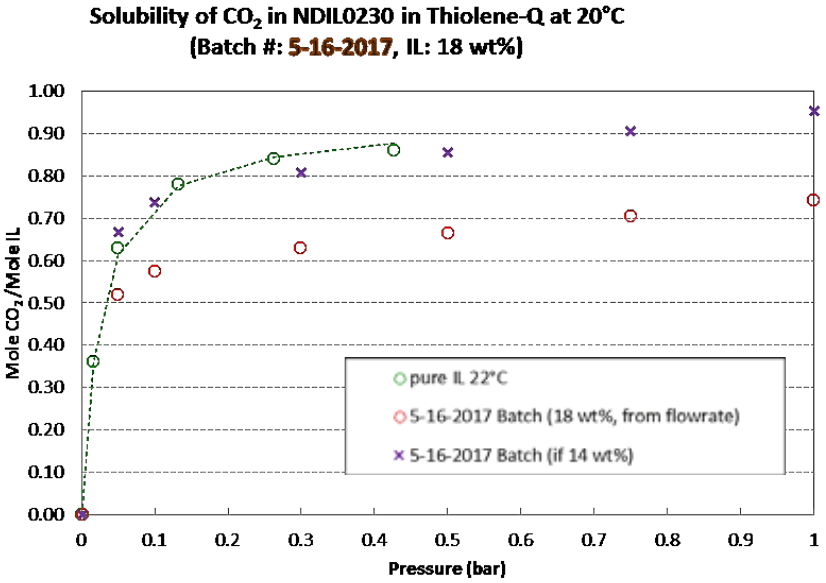

Figure 12: Solubility of CO_2 in NDIL0230 encapsulated in Thiolene-Q at 20 °C (batch produced on 5/16/17). For these measurements the capsules had been evacuated to remove all water. The uptake has been corrected for physical dissolution in the polymer shell material (**Figure 5**). The IL content of the dried shells should be 18 wt% based on the flow rates in the microfluidic device. The graph also shows that the uptake matches the expected result better if the actual IL content were 14 wt%.

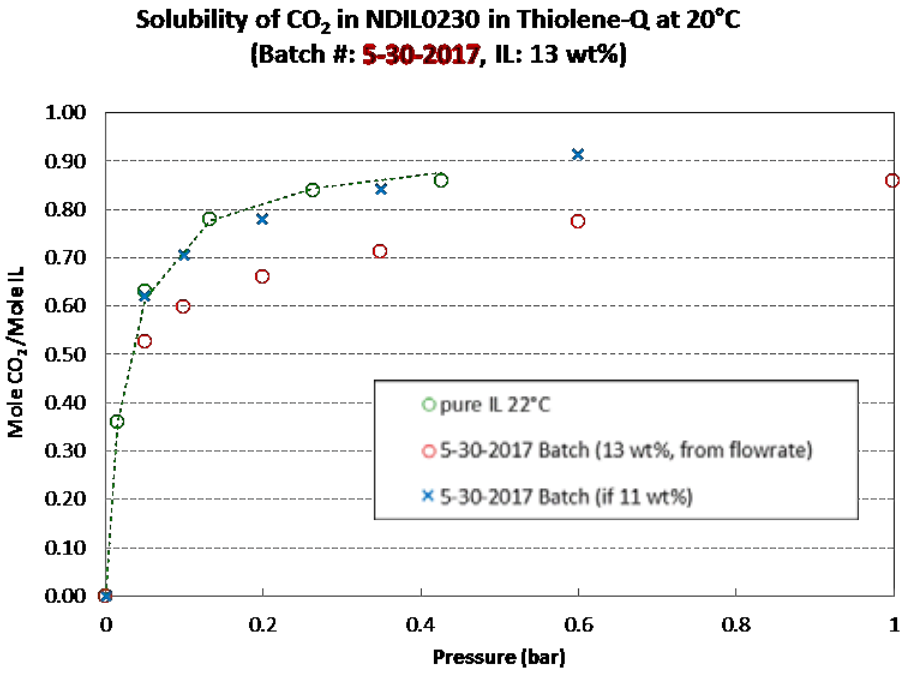

Figure 13: Solubility of CO_2 in NDIL0230 encapsulated in Thiolene-Q at 20 °C (batch produced on 5/30/17). For these measurements the capsules had been evacuated to remove all water. The uptake has been corrected for physical dissolution in the polymer shell material (**Figure 5**). The IL content of the dried shells should be 13 wt% based on the flowrates in the microfluidic device. The graph also shows that the uptake matches the expected result better if the actual IL content were 11 wt%.

In July and August 2017, we received several small samples of NDIL0230 encapsulated in Thiolene-Q from LLNL. We measured the CO_2 capacity for these samples at room temperature as a function of pressure for each sample in the Hiden gravimetric microbalance. For all samples, the CO_2 uptake was consistently 10% lower than expected based on the core and shell flow rates provided by LLNL. This small discrepancy may be attributed to some percentage of empty shells. The uptake data for one of these samples are shown below in **Figure 14**. The data have been corrected for the physical solubility of CO_2 in the polymer shell material, which we had measured previously. Based on the flow rates used by LLNL in the microfluidic device, the dried capsules should contain 10 wt% IL. As seen in **Figure 14**, the CO_2 uptake is about 10% low when compared to pure liquid IL. However, if the IL content was actually about 9 wt% (due to some empty shells), the capacity would match the expected values quite well. Whether 9 wt% or 10 wt%, this percentage of active ingredient is still too low for practical use.

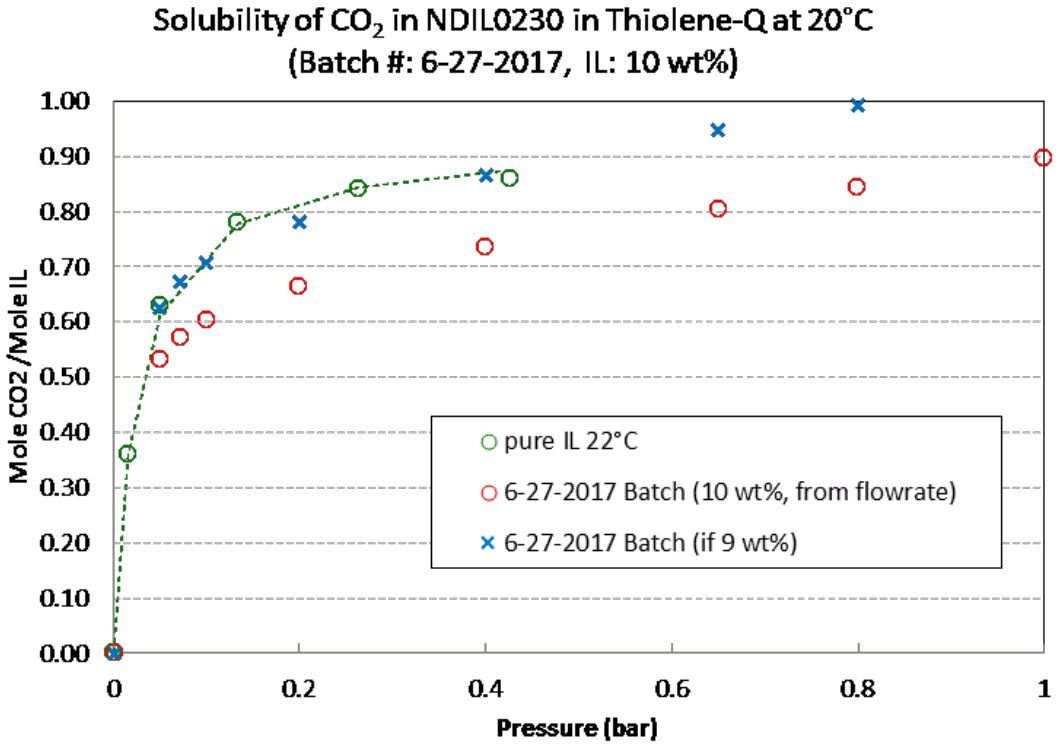

Figure 14: CO_2 capacity of NDIL0230 encapsulated in Thiolene-Q at 20 ºC. Based on the flowrates from the microfluidic device the capsules should contain 10 wt% IL, but the uptake matches the pure IL capacity better if the content is 9 wt% IL. This indicates the presence of some empty or broken shells.

Subsequent improvements in the production of capsules of NDIL0230, described under Task 3.0 above, resulted in the production of several small samples of NDIL0230 encapsulated in Thiolene-Q by LLNL with higher NDIL0230 content. We measured CO_2 uptake at room temperature as a function of pressure for three of the samples. We noted that there was something wrong with the 7/28/17 sample. The uptake was low and NMR confirmed very small amounts of IL in the shells. However, the CO_2 uptake for the two samples from 7/27/17 and 8/3/17 matched the expected values. The 7/27/17 sample was a mixture of capsules with 18 wt% IL and 21 wt% IL, resulting in an average of 19 wt% NDIL0230 content for the sample tested. The CO_2 capacity results, corrected for physical uptake by the shell material, for this sample are shown in **Figure 15**. The measured uptake matches the expected values from the pure IL measurements, indicating that previous problems with the formation of empty capsules had been resolved. Results for the 8/3/17 sample, corrected for physical uptake by the shell material, are shown in **Figure 16**. Based on the flow rates in the microfluidic device, the dry weight content of these capsules should be 40 wt% NDIL0230, which is sufficiently high for use in a practical absorber unit. The CO_2 capacity matches the expected values based on comparison with the CO_2 uptake of the pure IL, once again indicating that previous problems with the production of empty shells has been successfully resolved.

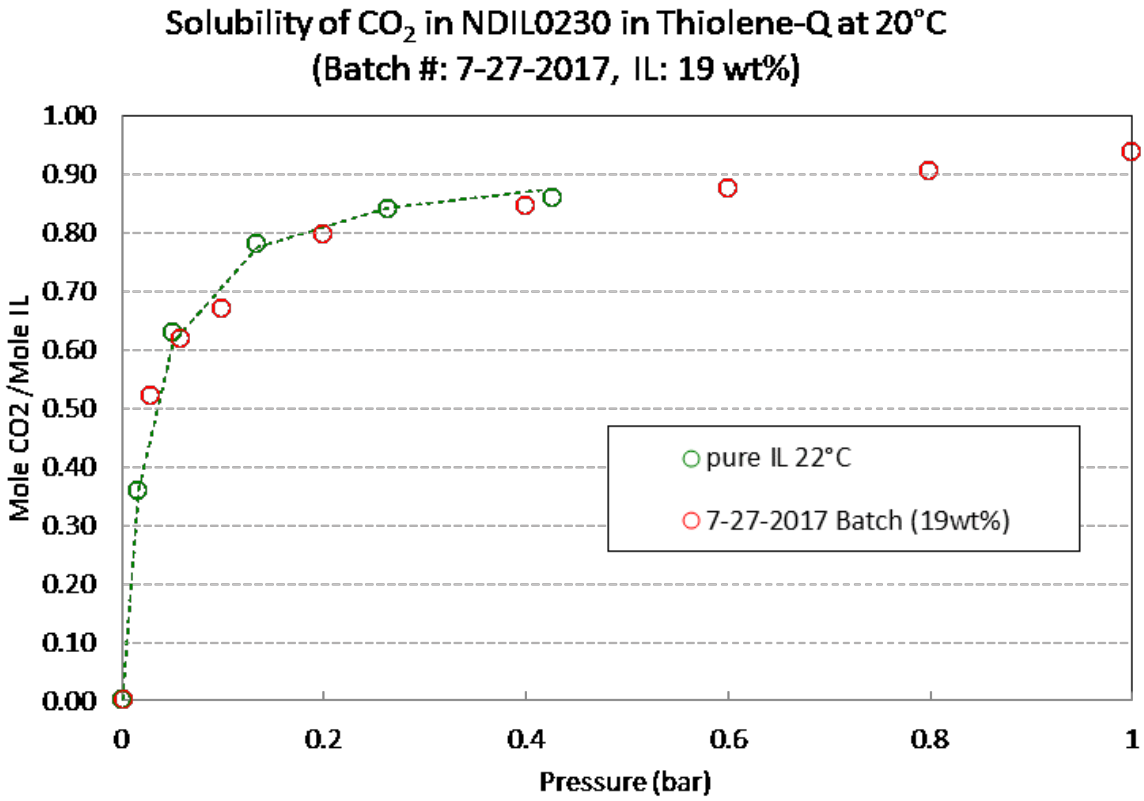

Figure 15: CO_2 capacity of NDIL0230 encapsulated in Thiolene-Q at 20 ºC. The capacity is consistent with pure IL uptake values based on an average IL content of 19 wt%, as indicated by the flow rates used in the microfluidic device.

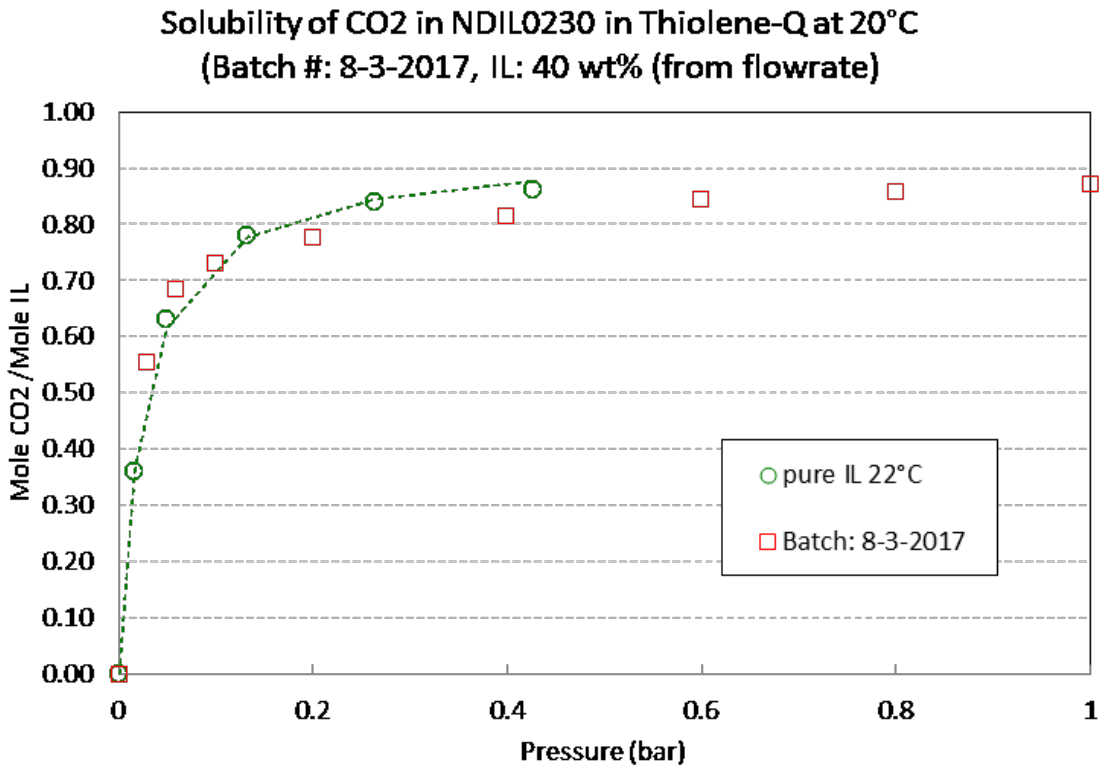

Figure 16: CO_2 capacity of NDIL0230 encapsulated in Thiolene-Q at 20 ºC. The capacity is consistent with pure IL uptake values based on an IL content of 40 wt%, as indicated by the flow rates used in the microfluidic device.

Subtask 4.2 – Mechanical and dynamic particle property testing

All work on this subtask was completed in BP1.

Task 7 - Mass transfer estimates

This task has been completed. We determined that, for both the fluidized bed and the packed bed, internal mass transfer resistance controls the CO2 uptake. That is, there is no significant effect of the gas fluidization velocity on the mass transfer coefficient.

Subtask 7.1 – Mass transfer for fluidized bed of IL microcapsules

We have performed experiments to estimate mass transfer coefficients in the fluidized bed, first with capsules filled with aqueous sodium carbonate solutions and then some initial tests with NDIL0309 capsules. These results are described below.

a. Capsules filled with aqueous sodium carbonate solution

Mass transfer experiments were designed to study transient absorption starting with fully regenerated capsules. The bed of carbonate filled capsules was initially fluidized with pure nitrogen at the chosen flow rate. Then the gas source was then changed to the designated inlet concentration of carbon dioxide. One such transient absorption experiment is shown in **Figure 17**, which produced an average mass transfer coefficient, k, of 0.00246 cm/s.

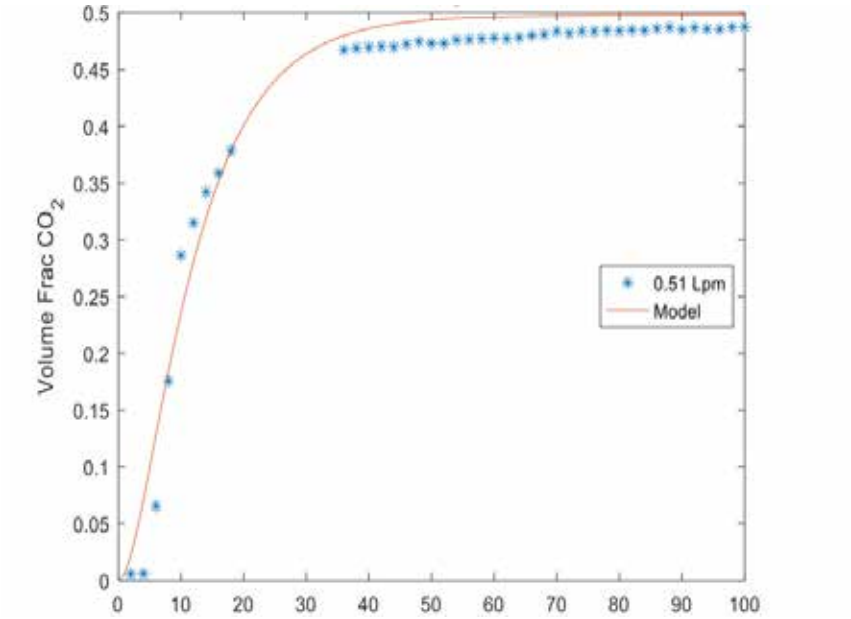

Figure 17: Volume of CO_2 absorbed vs. time (sec) as measured in transient absorption test of regenerated capsules.

The complete set of experiments covered the range of gas flow from 0.5 to 1.2 l/min, over which the bed was expanding to become fully fluidized. The inlet CO_2 concentration was varied from 20 to 50 vol% CO_2. Different total solids loadings were used. **Table 2** shows that there is no significant effect of inlet gas concentration or gas flow rate on the mass transfer coefficients. Most importantly, the mass transfer coefficients are substantially lower, by a factor of 10^{-3}, than what would be expected for either a packed bed or a fluidized bed if external resistance controlled the absorption. **Table 3** shows that the $K_{External}$ mass transfer coefficient values range from ~12 to 22 cm/s for our capsules under these flow conditions.

Table 2: CO_2 uptake by aqueous sodium carbonate capsules

C_{in} (%)	C_{out} (%)	Particle Mass (g)	Flow Rate (Lpm)	k (cm/s)
22.1	15.3	22.6	0.92	2.31E-03
22.7	11.8	11.5	1.0	1.97E-02
22.8	10.3	5.3	1.15	2.83E-02
49.8	34.2	11.5	0.51	2.46E-03

Table 3: Mass transfer coefficients for aqueous sodium carbonate capsules

	0.51 Lpm	0.68 Lpm	0.92 Lpm	1 Lpm	1.15 Lpm
k (cm/s)	2.56E-03	1.32E-02	2.31E-03	1.97E-02	2.83E-02
$K_{External}$ (cm/s)	11.7	14.3	18	19.4	21.7

Thus, internal mass transfer controls the process. We can therefore estimate an *internally* controlled *k*. Using the diffusivity of CO_2 into a sodium carbonate in water solution as being of the order of 10^{-5} cm^2/s, and a sphere diameter of 550 μm, gives an internally controlled mass transfer coefficient of ~3 x 10^{-4} cm/s. Thus, the data show conclusively that external mass transfer resistance is negligible. Further, they are suggestive that the polymer coating is likewise not contributing a significant resistance to mass transfer.

b. Thiolene-Q Capsules filled with NDIL0309

Measurements of CO_2 absorption into IL filled capsules were conducted over a range of temperatures and flow rates. The procedure involved starting with initially CO_2 depleted capsules, setting the flow rate to induce fluidization, and then switching the inlet concentration to the prescribed CO_2 concentration. The experiment was conducted as a transient absorption process. **Figure 18** shows a typical run. Here, the outlet CO_2 concentration is being measured.

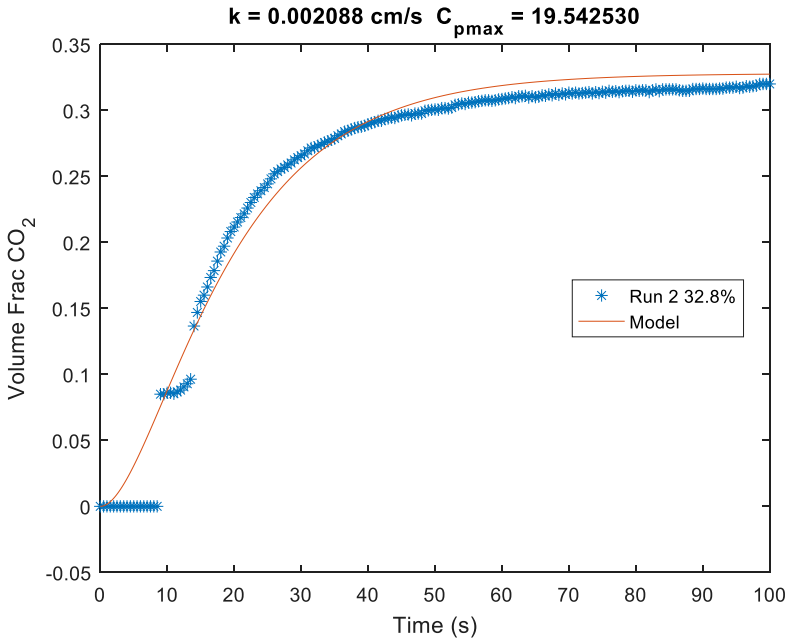

Figure 18: Volume fraction of CO_2 absorbed vs. time (sec) for Thiolene-Q capsules filled with NDIL0309.

Our initial experiments showed some CO_2 absorption but the total uptake (mol ratio in the **Table 4**, below) was less than 1/3 of the expected loading of approximately 1 mole of CO_2 absorbed for each mole of IL in the capsules.

Table 4: CO_2 uptake results

Composition (vol % CO2)	Pco2 (bar)	Temp (C)	Absoption Time (s)	Absorption Amount (L CO2)	(mol CO2)	Regeneration Amount (L CO2)	(mol CO2)	Regen Temp (C)	mol ratio	k (cm/s)
23.53	0.256	40	156	0.046	0.0019	0.143	0.00599	72	0.291	3.51E-04
27.26	0.335	80	824	0.258	0.0108	0.136	0.00569	74	0.277	6.34E-05
18.45	0.217	65	1257	0.265	0.0111	0.127	0.00532	54	0.258	6.68E-04
23.99	0.278	60	644.5	0.115	0.0048	0.115	0.00481	63	0.234	1.98E-04
46.37	0.568	79	1003	0.560	0.0234	0.149	0.00624	71	0.303	2.79E-05

To address this issue, we continued to refine our experiments. We discovered that we needed a higher regeneration temperature to fully desorb the CO_2. Further we also found that a higher temperature for the inlet gas allowed more efficient absorption. As seen in **Table 5**, below, the most current experiment series has attained loadings (mol ratio) of 0.6-0.7, which we deem acceptable. The experiments shown in Table 5 were performed sequentially with the same batch of Thiolene-Q encapsulated NDIL0309 particles. They were performed in the laboratory scale unit. Therefore, these runs demonstrate the recyclability of Thiolene-Q encapsulated NDIL0309 capsules. The mol ratio in the

second to last column of Table 5 demonstrates consistent CO_2 removal of 0.66 $\pm$ 0.02 mol CO_2/mol PCIL (and therefore consistent CO_2 uptake) over five cycles.

Table 5: Effect of regeneration temperature on CO_2 uptake

Total Flow Rate (Lpm)	Composition (vol % CO_2)	P_{Co2} (bar)	Temp (C)	Absorption Time (s)	Regen-eration Amount (L CO_2)	(mol CO_2)	Regen Temp (C)	mol ratio	k (cm/s)
3.3	45.67	0.547	71	1236	0.229	0.0096	114	0.65	1.5E-05
3.3	44.55	0.537	73	433	0.224	0.0094	106	0.64	2.2E-04
3.3	45.93	0.561	78	733	0.23	0.0096	109	0.66	3.1E-05
3.3	44.74	0.533	69	673.5	0.228	0.0095	108	0.65	8.8E-05
3.3	45.22	0.542	71	356	0.243	0.0101	114	0.69	1.0E-04

Subtask 7.2 – Mass transfer for packed bed of IL microcapsules

Our reason for considering the possibility of using a packed bed for the absorption process at the proposal stage was because the durability of the capsules, when subjected to the stresses of a fluidized bed, was not known. All experiments to date, as designated in the original work plan, have proven that capsules are sufficiently robust to withstand a fluidized absorption process. Since this is the case, there is no reason to run the absorber as a packed bed as it would limit heat removal, gas mixing and lessen the effective contact area between the gas and solids.

However, we made some runs with the capsules in which we simulated a packed bed by placing a screen on the bed and thus preventing fluidization. As expected, since the mass transfer resistance is inside the capsules, the mass transfer coefficients for a packed compared to those in a fluidized bed are about the same. However, we found that we could not achieve as high of a loading in the packed compared to the fluidized bed. This is likely because the capsules pack in such a way as to create some dead space in the bed. However, since we don't intend to use a packed bed in the commercial embodiment of this process, these problems are not significant.

Table 6: Packed bed vs. fluidized bed results

Total Flow Rate (Lpm)	Composition (vol % CO_2)	P_{CO2} (bar)	Temp (C)	Regeneration Amount (L CO_2)	(mol CO_2)	Regen Temp (C)	mol ratio	k (cm/s)
(Packed) 2.4	43.5	0.519	70	0.07	0.0029	100	0.23	2.94E-04
(Fluidized) 3.3	44.55	0.537	73	0.22	0.0094	106	0.64	2.17E-04

Task 8.0 – Effect of impurities (for ILs in silicone microcapsules)

Subtask 8.1 - Measurements of solubility and chemistry of exposure of liquid ILs to SO_2, NO_x, and water

Post-combustion flue gas contains a variety of other components besides CO_2 and N_2. Of particular concern is SO_2, NO_x and water. In order to study the effect of SO_2 and NO_x on the IL, PCIL and encapsulated materials, we had to set up a gravimetric microbalance system in a floor length hood. The system is shown in **Figure 19**.

Figure 19: Photographs of Rubotherm gravimetric microbalance system in hood to determine the effect of SO_2 and NO_x on NDIL0230, NDIL0309 and encapsulated versions of these materials.

NO_x

We measured the solubility of NO in NDIL0230 at 20 °C and pressures to 12 bar. The results are shown in **Figure 20**. After the sample was degassed, it was removed from the apparatus. After desorption, the sample had changed color (see **Figure 21**) and we observed changes in the ^{1}H NMR spectrum, leading us to conclude that there is unwanted chemistry taking place.

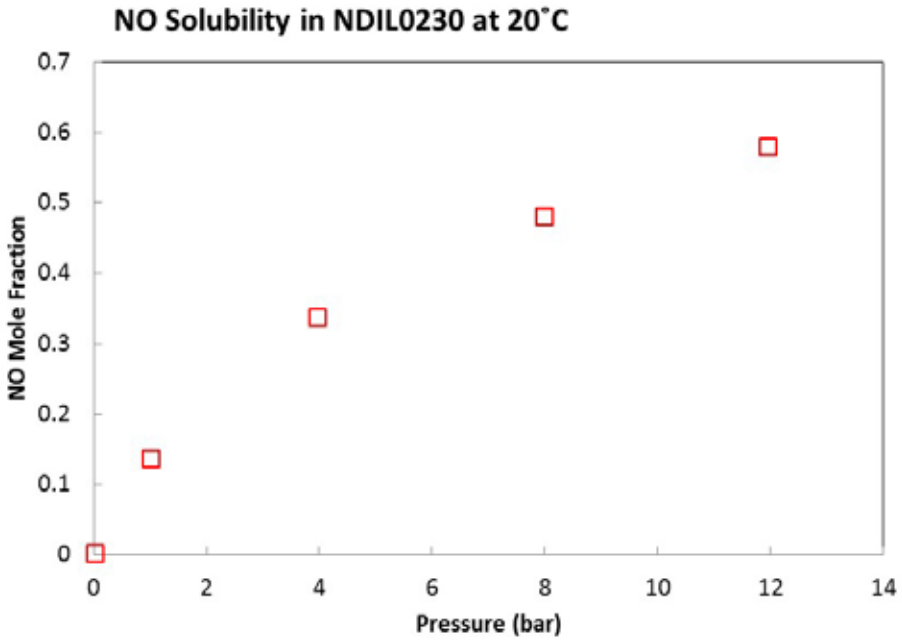

Figure 20: Solubility of NO in NDIL0230 at 20 °C

Figure 21: The color of the NDIL0230 changed after exposure to NO. The left NMR tube is pure NDIL0230 in DMSO. The right NMR tube is the NDIL0230 after exposure to NO, followed by pulling vacuum, in DMSO.

It is not possible to perform the same experiments with NDIL0309 because it is a solid, with a melting point of 166 °C. It is only after it reacts with CO_2 that it is a liquid at operating conditions. However, as mentioned above, we found an IL, NDIL0001, which dissolves significant amounts of NDIL0309. The solubility of NO in a mixture of 10 mol % NDIL0309 + 90 mol % NDIL0001 is shown in **Figure 22,** in comparison to the values

in NDIL0230 and pure NDIL0001. Obviously, the NO uptake in all three ILs is quite high. More importantly, ^{1}H NMR analysis of the mixture shows significant degradation of the NDIL0309 after exposure to NO. By contrast, NO dissolves reversibly in NDIL0001, without any changes in the ^{1}H NMR spectrum after exposure to NO. Of course, NDIL0001 is not an IL capable of reversible CO_2 capture. In addition, the NDIL0309 + NDIL0001 mixture changes color (clear to yellowish) and forms a solid precipitate after exposure to NO, as shown in **Figure 23.**

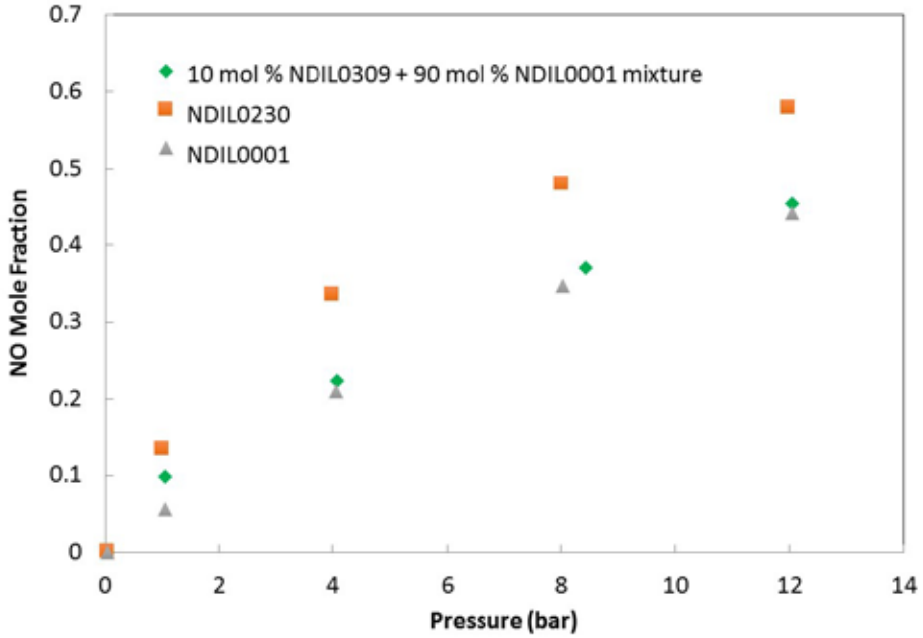

Figure 22: Solubility of NO in NDIL0230, NDIL0001 and a mixture of NDIL0309 and NDIL0001 at 22 °C.

Figure 23: Photographs of NDIL0309 + NDIL0001 mixture before and after exposure to NO at 22 °C.

Based on these results, we conclude that both NDIL0230 and NDIL0309 react irreversibly with NO. As a result, any NO_x impurities in the flue gas would result in degradation of the IL or PCIL.

SO_2

We measured the SO_2 uptake in NDIL0230 at room temperature (**Figure 24**), as well as the SO_2 uptake in a mixture of NDIL0309 and NDIL001 at room temperature (**Figure 25)**. Initial indications were that only part of the SO_2 absorption was reversible. Cycling of SO_2 sorption in a mixture of NDIL0309 and NDIL0001 (**Figure 26**) showed that SO_2 reacts with the ILs/PCILs irreversibly and this was confirmed by ^1H NMR analysis.

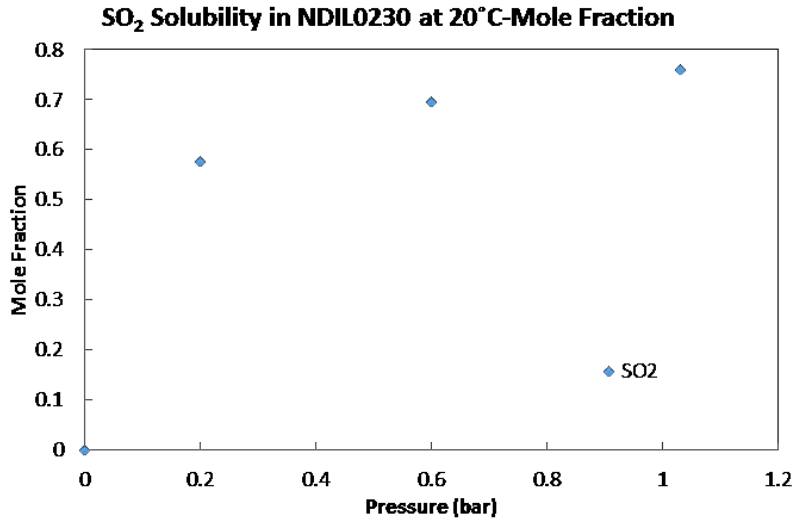

Figure 24: Solubility of SO_2 in a NDIL0230 as a function of pressure at 20 °C.

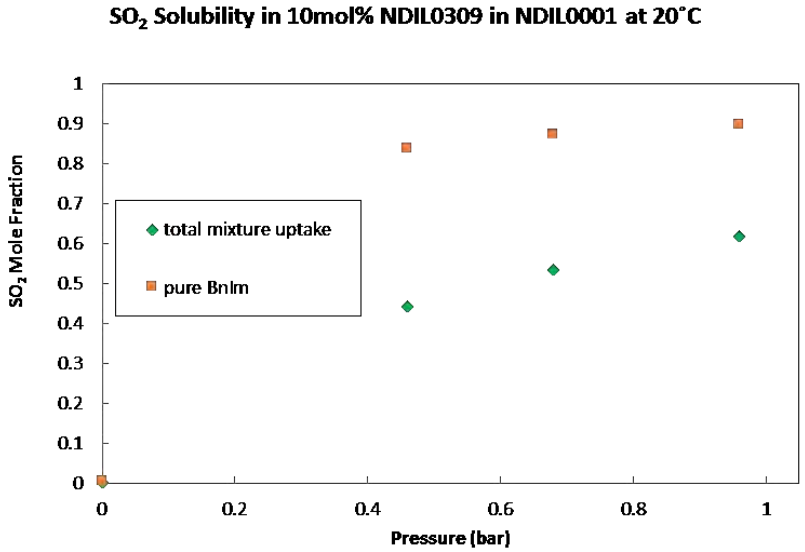

Figure 25: Solubility of SO_2 in a mixture of 10 wt% NDIL0309 in NDIL0001 as a function of pressure at 20 °C. The estimated solubility of the SO_2 in just the NDIL0309 was determined by subtracting the known SO_2 solubility in NDIL0001.

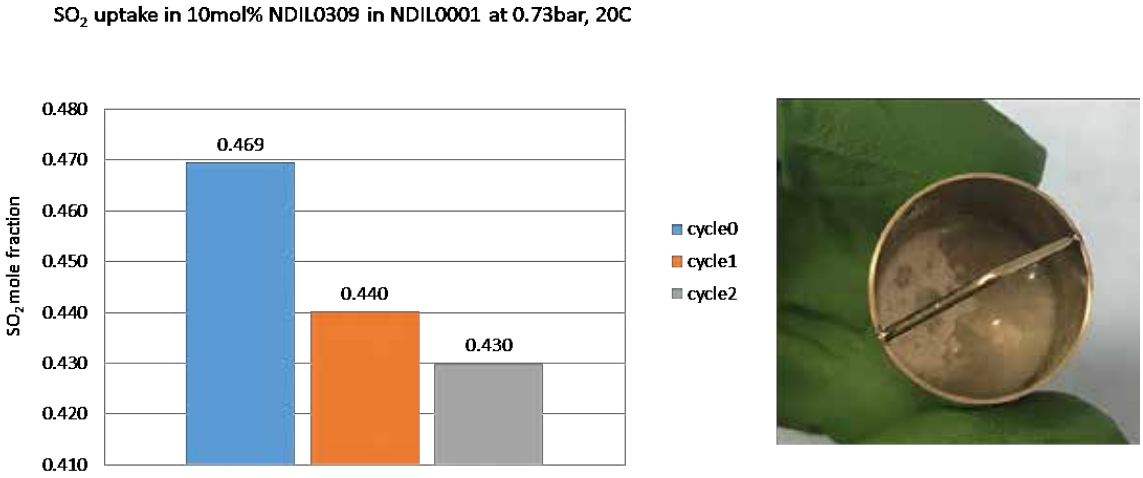

Figure 26: Three cycles of the solubility of SO_2 in a mixture of 10 wt% NDIL0309 in NDIL0001. The capacity decreased so the cycling experiment was discontinued and the sample observed visually, indicating formation of precipitates.

Water

In the Topical Report for BP1, we showed the results for the reprotonation of NDIL0230 and NDIL0309 at room temperature as measured by ^{1}H NMR spectroscopy. This only occurs in the presence of CO_2; no reprotonation of the anion occurs when contacted with just water. (Recall that NDIL0231 was eliminated in the first year of this project since it did reprotonation just in the presence of water). In our technique to measure the reprotonation, we follow the amount of water present as a function of time, since the reprotonation of the anion and formation of bicarbonate consumes water. We found that water consumption, with the associated reprotonation of the anion and formation of bicarbonate, occurs very quickly (i.e., on the order of minutes). Since the reprotonated anion is large and, therefore, unlikely to diffuse out through the Thiolene-Q shell, in this Subtask we have focused on determining if the reaction of the IL or PCIL anion with CO_2 and water is reversible.

Reversibility is measured in the reaction cell of the CO_2 uptake volumetric apparatus. A sample of the NDIL0230 or NDIL0309 and H_2O (4 mol of H_2O/ mol IL or PCIL) was placed in the apparatus and the CO_2 uptake measured in the standard fashion at 22 ^{O}C. After the sample has reached equilibrium, the IL or PCIL was regenerated under vacuum (at 60 ^{O}C for three days for the IL and 80 ^{O}C for three days for the PCIL) to ensure complete removal of both CO_2 and water (recall that the IL and PCIL are quite hygroscopic). Afterwards water was added (4 mol of H_2O/ mol IL) to start another cycle. Obviously, complete water removal would not be necessary in a commercial CO_2 capture and regeneration process. Thus, the long regeneration time is simply a component of the laboratory experimental procedure to accurately quantify the recyclability.

The recyclability results for NDIL0230 are shown in **Figure 27**. As shown in the figure, the CO_2 uptake of the wet IL is roughly the same as the pure dry IL. The uptake in the second cycle drops about 7% but then remains completely steady within experimental uncertainty for the next three cycles. This indicates that both the reaction of CO_2 with the

anion (as shown previously with CO_2 uptake recyclability tests with the dry IL), and the reprotonation reaction and formation of bicarbonate, are completely reversible. They do not result in degradation of the IL.

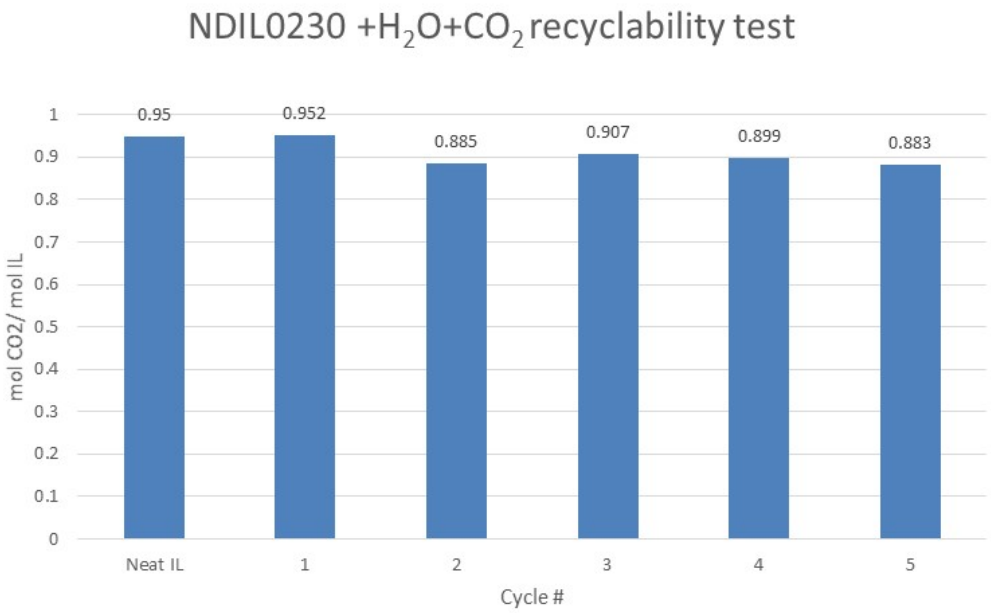

Figure 27: Recyclability of NDIL0230 in the presence of water (4 mol of H_2O/ mol IL), as determined by CO_2 uptake at 22 ^{O}C and ~1 bar of CO_2 pressure.

The equivalent recyclability results for NDIL0309 are shown in **Figure 28.** These experiments were also done at room temperature, although we anticipate that absorption with NDIL0309, the phase change IL, would take place at higher temperature (e.g., 70 or 80 ^{O}C), where we have shown that the PCIL absorbs very little water so that it is solid before it reacts with CO_2 and the process can take advantage of the energy savings provided by the phase change to a liquid when the PCIL reacts with CO_2. Not surprisingly, the CO_2 uptake of the wet (4 mol of H_2O/ mol PCIL) NDIL0309 at 22 ^{O}C is a bit higher than that of the dry PCIL at 70 ^{O}C. After the first cycle, the CO_2 capacity drops about 7% but then remains constant within experimental uncertainty for the next three cycles. Like the NDIL0230, this indicates that both the reaction of CO_2 with the anion (as shown previously with CO_2 uptake recyclability tests with the dry IL), and the reprotonation reaction and formation of bicarbonate, are completely reversible. They do not result in degradation of the PCIL.

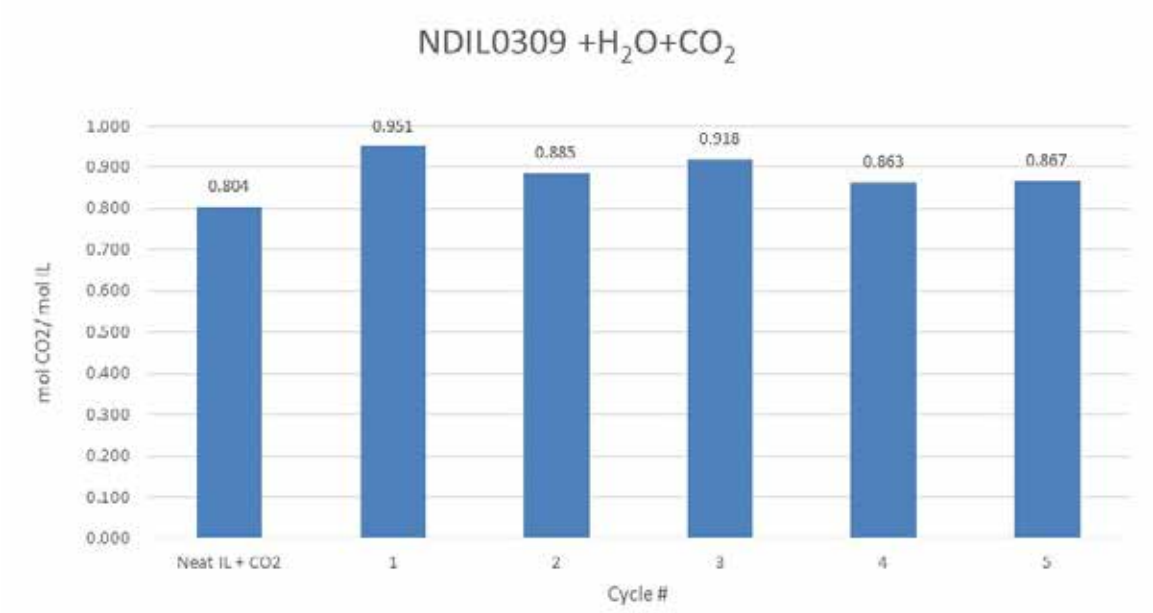

Figure 28: Recyclability of NDIL0309 in the presence of water (4 mol of H_2O/ mol IL), as determined by CO_2 uptake at 22 ^{O}C and ~1 bar of CO_2 pressure.

The work for Subtask 8.1 is complete. We have determined that SO_2 and NO react irreversibly with both NDIL0230 and NDIL0309. Therefore, the CO_2 capture unit would need to be positioned after the flue gas desulfurization unit and the NOx reduction unit. By contrast, we have shown that the reaction of the IL or PCIL with CO_2 in the presence of water is completely reversible and recyclable. Therefore, the presence of water in the flue gas is not a showstopper. The development of water impermeable shells is not necessary.

Subtask 8.2 – Effect of SO_2 and NO_x on IL microcapsules

$\underline{NO_x}$

We have measured the effect of NO on NDIL0309 in Thiolene-Q capsules (**Figure 29**. Not surprisingly, on an IL basis, the solubility of NO in the capsules is similar to the solubility of NO in the mixture of NDIL0309 and NDIL0001, shown in **Figure 22**. Based on the results for the liquid mixture of NDIL0309 and NDIL0001 (Subtask 8.1), we anticipated that the NO will react irreversibly with NDIL0309. This is indeed the case. The material in the capsules changes color from clear to brown, as shown in **Figure 30**. ^{1}H NMR analysis of the core material before and after the NO solubility test confirmed degradation of the NDIL0309.

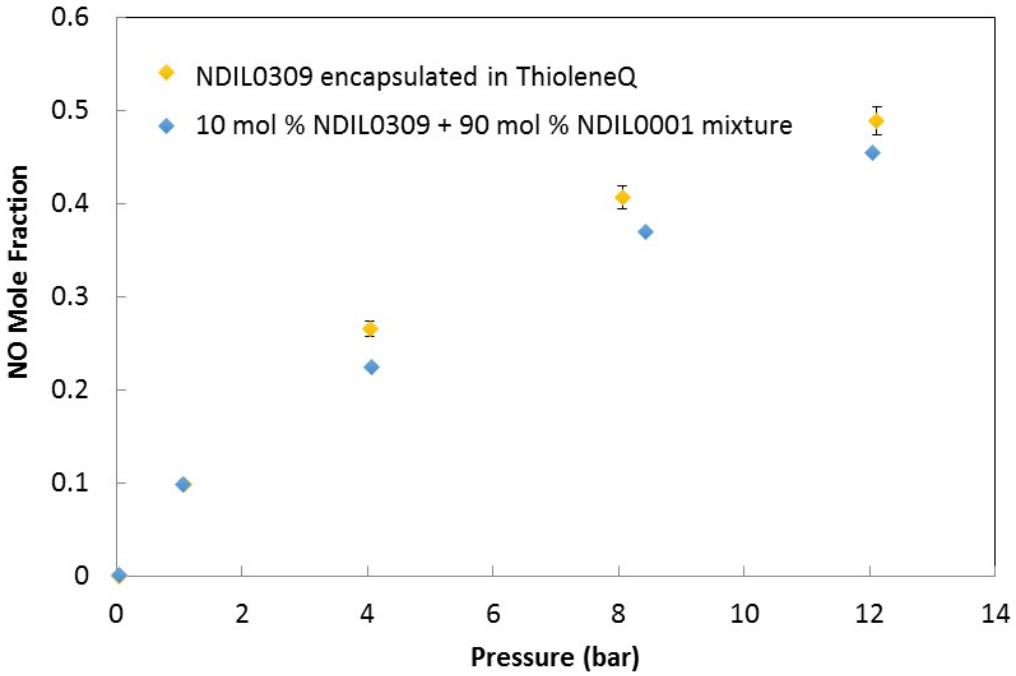

Figure 29: Solubility of NO in NDIL0309 encapsulated in Thiolene-Q shells at 22 °C.

Figure 30: NDIL0309 encapsulated in Thiolene-Q before and after exposure to NO at 22 °C.

We measured the uptake of NO at room temperature as a function of pressure for samples of NDIL0230 - Thiolene-Q for capsules received from LLNL on 5/30/2017. The NOuptake by this sample, which is nominally 11 wt% IL, is shown in **Figure 31**. These experiments were performed in the Rubotherm microbalance that was assembled in a floor length hood with appropriate exhaust scrubbing and safety monitoring. The NO uptake was not reversible. Treatment with NO produced a color change of the capsules. Post-analysis by NMR spectroscopy confirmed irreversible degradation of the IL.

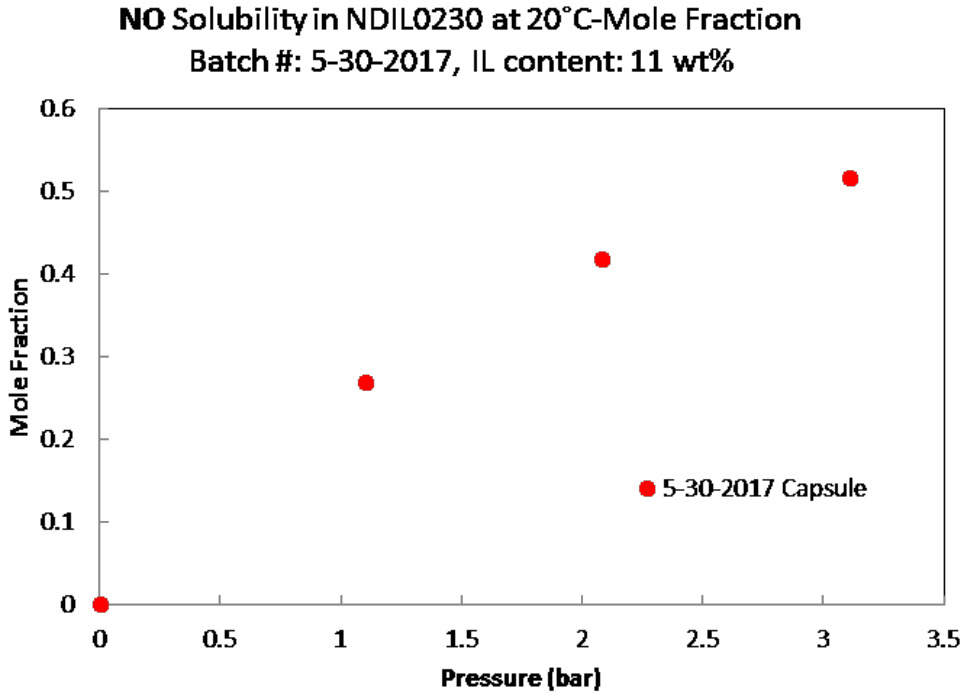

Figure 31: Uptake of NO by encapsulated NDIL0230 at 20 ºC. The capsules nominally contain 11 wt% IL. The uptake was not reversible.

SO_2

The SO_2 solubility in NDIL0309 encapsulated in Thiolene-Q was measured at 20 °C as a function of pressure. The uptake was cycled and the values for the second cycle were significantly lower than the first cycle, as shown in **Figure 32**. The capsules had turned from clear to dark brown, as shown in **Figure 33**. ^{1}H NMR of the contents of the shells confirmed decomposition and unwanted reactions after exposure to SO_2.

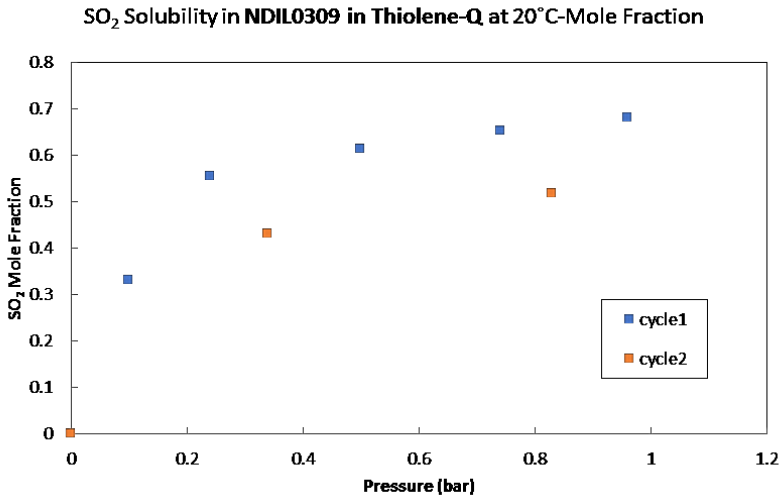

Figure 32: Solubility of SO_2 in NDIL0309 encapsulated in Thiolene-Q at 20 °C. The capacity decreases for the second cycle due to irreversible reaction between the SO_2 and NDIL0309.

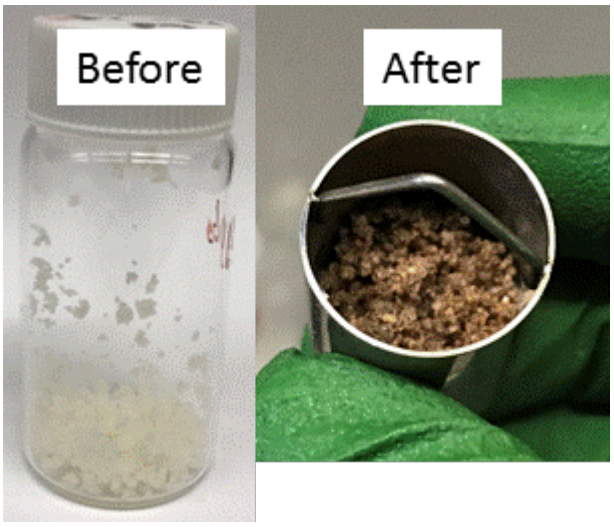

Figure 33: Photographs of Thiolene-Q encapsulated NDIL0309 particles before and after exposure to SO_2.

We measured the uptake of SO_2 at room temperature as a function of pressure for samples of NDIL0230 - Thiolene-Q for capsules received from LLNL on 5/30/2017. The SO_2 uptake by this sample, which is nominally 11 wt% IL, is shown in **Figure 34**. These experiments were performed in the Rubotherm microbalance that was assembled in a floor length hood with appropriate exhaust scrubbing and safety monitoring. The uptake was not reversible, resulting in color change of the capsules and post analysis by NMR spectroscopy confirmed irreversible degradation of the IL.

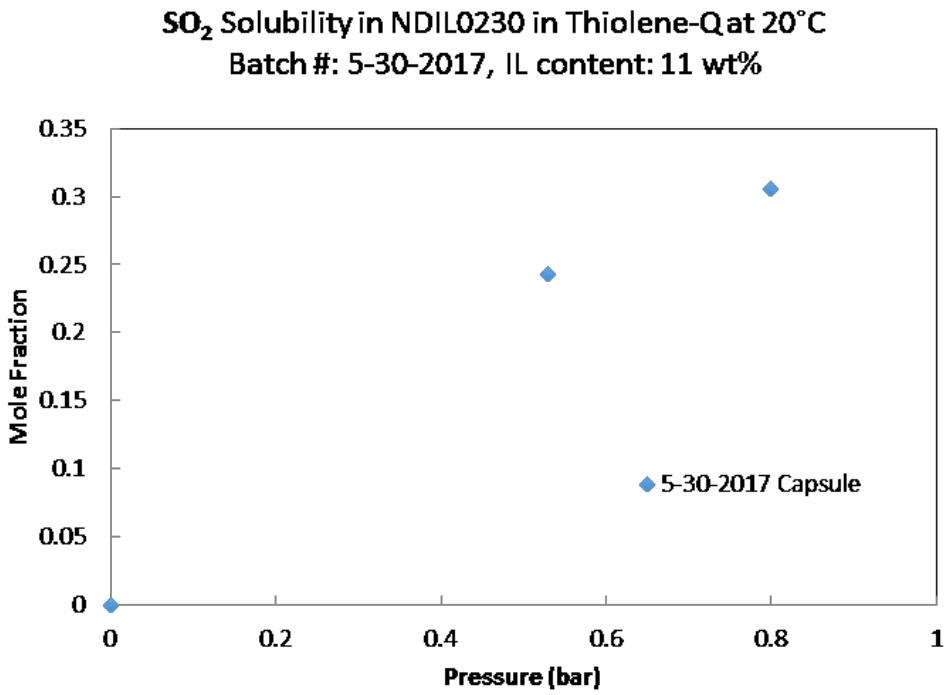

Figure 34: Uptake of SO_2 by encapsulated NDIL0230 at 20 ºC. The capsules nominally contain 11 wt% IL. The uptake was not reversible.

Based on all of these results, we conclude that the unwanted chemistry occurring between the IL and the PCIL with both SO_2 and NO occurs in the free material as well as in the encapsulated material.

Subtask 8.3 – Effect of water on IL microcapsules

The effect of water on the CO_2 uptake of NDIL0309 encapsulated in Thiolene-Q was investigated in the volumetric apparatus, as described under Subtask 8.1. Care was taken to agitate the capsules gently in order to ensure that they do not break. As shown in Subtask 8.1, the uptake with 4 moles water present per mole of NDIL0309 increases the CO_2 uptake from about 0.8 moles of CO_2/mole of IL to 0.95 moles CO_2/mole of IL. Likewise, the CO_2 uptake in the encapsulated NDIL0309 is higher when water is present. The experiments were conducted at room temperature since the NDIL0309/water mixture is a liquid at these conditions. In addition, we completed five cycles of the effect of water on encapsulated NDIL0309 in the presence of CO_2, and these results are shown in **Figure 35**. There is only a small reduction in the capacity over the five cycles. We attribute this to difficulty in removing all the CO_2 from the solid at room temperature, since both water and CO_2 is removed during the regeneration. ^{1}H NMR analysis of the core material after cycling confirmed complete reversibility and no degradation.

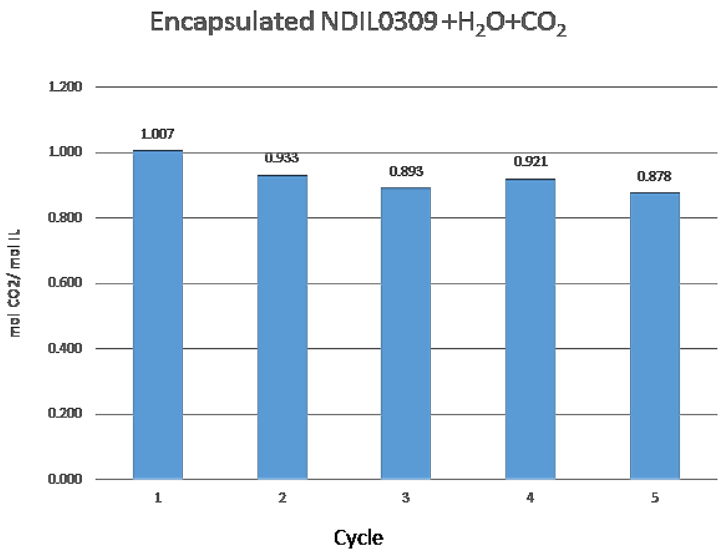

Figure 35: Solubility of CO_2 in NDIL0309 encapsulated in Thiolene-Q at room temperature and in the presence of 4 moles of water per mole of IL. Cycling was achieved by heating to 80°C and pulling vacuum.

The effect of water on the CO_2 uptake of encapsulated NDIL0230 was determined using the volumetric apparatus, which requires approximately 2 g of IL. Since all samples received from LLNL up to this time were less than 2 or 3 g total weight (including water in the core and the shell mass), several samples of widely different IL contents had to be combined in order to perform these experiments. However, knowing the mass of each sample the average IL content was known. The experiments are done with 4 moles of water per mole of IL, which is freshly reintroduced into the sample after desorption under vacuum. As shown in **Figure 36** the initial CO_2 uptake (0.936 moles of CO_2 per mole of IL) was consistent with the uptake for the free IL in the presence of water and CO_2. After three cycles the uptake decreased by about 10%. It is possible that this small decrease is due to incomplete regeneration, rather than any actual degradation of the sample. At this point, the combined sample had to be removed from the apparatus for the move of our laboratory from the University of Notre Dame to the University of Texas at Austin. Two more absorption/desorption runs were performed this quarter at UT Austin. The absolute CO_2 uptake values are higher than expected based on the average IL content of the capsules. This is attributed to the fact that the samples had to be removed from the apparatus and put back in it after the move. There is some sample loss during this process. Since the capsules were a mixture of several very small batches from LLNL with varying amounts of NDIL0230 content, it is possible that some of the lower IL content capsules were lost. The capsules are somewhat sticky so they are not well mixed in the volumetric sorption vessel. For these measurements the capsules are not dusted with silica, which is the treatment used to enhance fluidization in the laboratory scale unit. More importantly for this subtask, the CO_2 uptake for Cycle 5 matched the value for Cycle 4 within experimental uncertainty; i.e., there was no loss in capacity due to cycling. While the experiment wasn't optimal because of sample removal and replacement as a result of the move, the results clearly satisfy the milestone requirements.

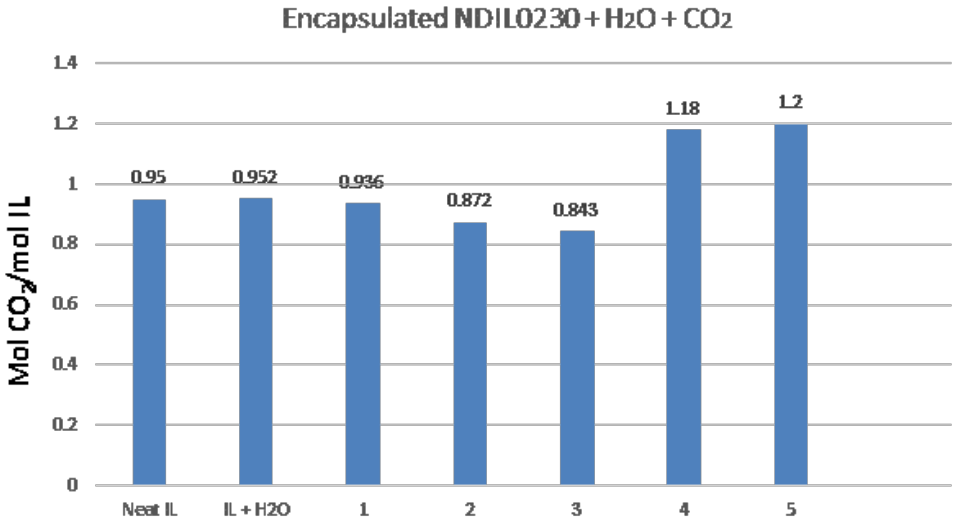

Figure 36: Recyclability of CO_2 uptake by encapsulated NDIL0230 in the presence of water. Cycles 1-3 were performed at the University of Notre Dame. Cycles 4 and 5 were performed at the University of Texas at Austin. The apparent increase in capacity is an artifact of having to remove the capsules from the apparatus for the move, as explained in the text.

Task 9.0 – Selection of top two ILs and synthesis of ~ 1 kg quantities of each

Subtask 9.1 – Synthesis and purification

The top two ILs selected are NDIL0309 (a PCIL) and NDIL0230 (an IL). We have >1 kg of NDIL0309 on hand from a previous DOE ARPAe project. We have analyzed the sample by ^{1}H NMR spectroscopy and the material retains its as-made purity. In Fall 2016, we synthesized and purified ~1 kg of new NDIL0230.

Subtask 9.2 – Physical property measurements

The density and viscosity of the kg batch of NDIL0230 that was synthesized and purified by 12/31/16 (Subtask 9.1) was measured in the quarter ending 3/31/17 and they match values for previous batches to our satisfaction, as shown in **Figure 37** and **Figure 38**.

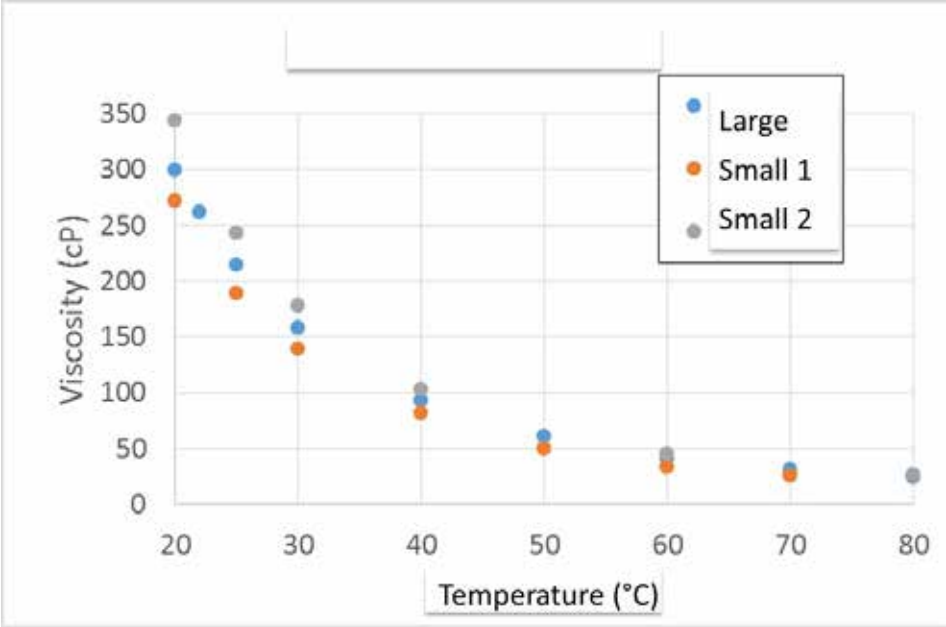

Figure 37: Viscosity of large batch of NDIL0230 in comparison to two previously synthesized small batches.

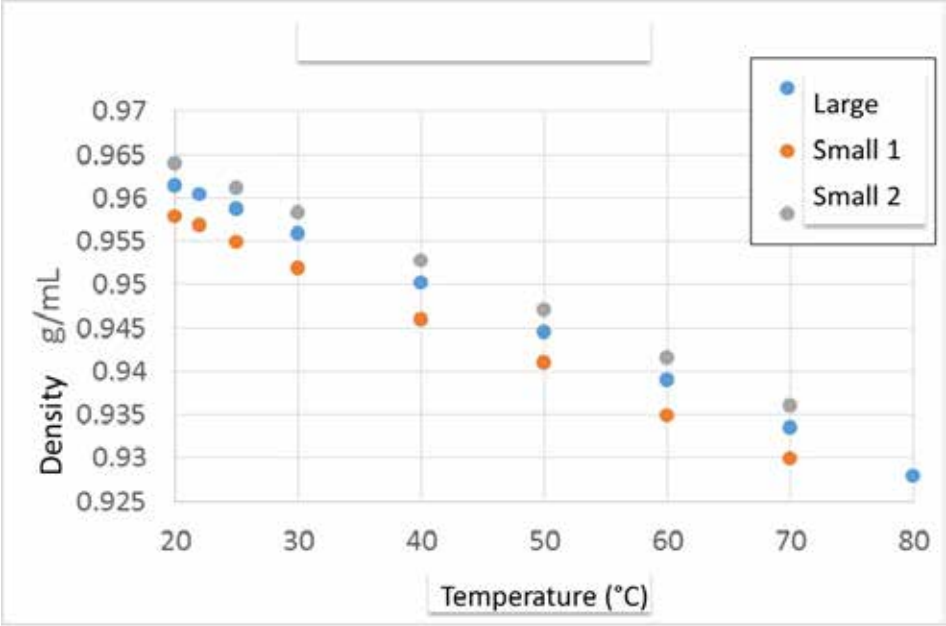

Figure 38: Density of large batch of NDIL0230 in comparison to two previously synthesized small batches.

Task 10.0 – Synthesis of large quantities (~1 kg) of encapsulated ILs

During BP 2, we pursued multiple options for production scale-up. In summary, NDIL0309 - Thiolene-Q capsules have been fabricated successfully in parallelized microfluidic chips. This is the scale-up method selected for NDIL0309 so Subtask 10.1 is complete for NDIL0309. This method resulted in the production of roughly a kg

(cumulative) of encapsulated NDIL0309 by the end of BP2 (9/30/17). Two methods were evaluated for scale-up for encapsulating NDIL0230. One was the parallelized microfluidic chip. The other method, using a vibrating nozzle and designated the in-air drop encapsulation apparatus (IDEA), has been chosen at the scale-up method for encapsulating NDIL0230. The target date for producing a kg quantity of encapsulated NDIL0230 is 12/31/17.

Subtask 10.1 – Identify scale-up method for ILs and PCILs

The most straightforward choice of scale-up method is to parallelize the type of microfluidic production that we used to make gram quantities of capsules. In general, this is achieved by using microfluidic chips with multiple devices etched into each chip. The LLNL team had meetings with three industrial chipmakers, Aline, Inc., Inzign Pte Ltd, and IMT. We currently use chips from Dolomite microfluidics, but price and turnaround time for those are a limitation. As a risk mitigation effort, we are also developing custom microfluidic chips with our collaborators at Harvard University, using laser etching on PMMA wafers. We made a first demonstration of continuous production with a candidate shell material (but not yet with an IL). Additional scale-up options for composite pellets were also considered, before settling on the parallel microfluidic production of encapsulated NDIL0309, as described below.

Parallel production of NDIL0309 - Thiolene-Q capsules have been successfully carried out with Dolomite's Telos system and is being used to produce the latest samples. (**Figure 39**). The system was quite stable with a minimum requirement of maintenance during an 8-hr production and generated ~ 60 g of dry capsules. This used one chip containing four devices. In practice, 3—6 such chips can be run simultaneously to produce 1 kg of capsules. This is the method that we have selected for producing large quantities of encapsulated NDIL0309.

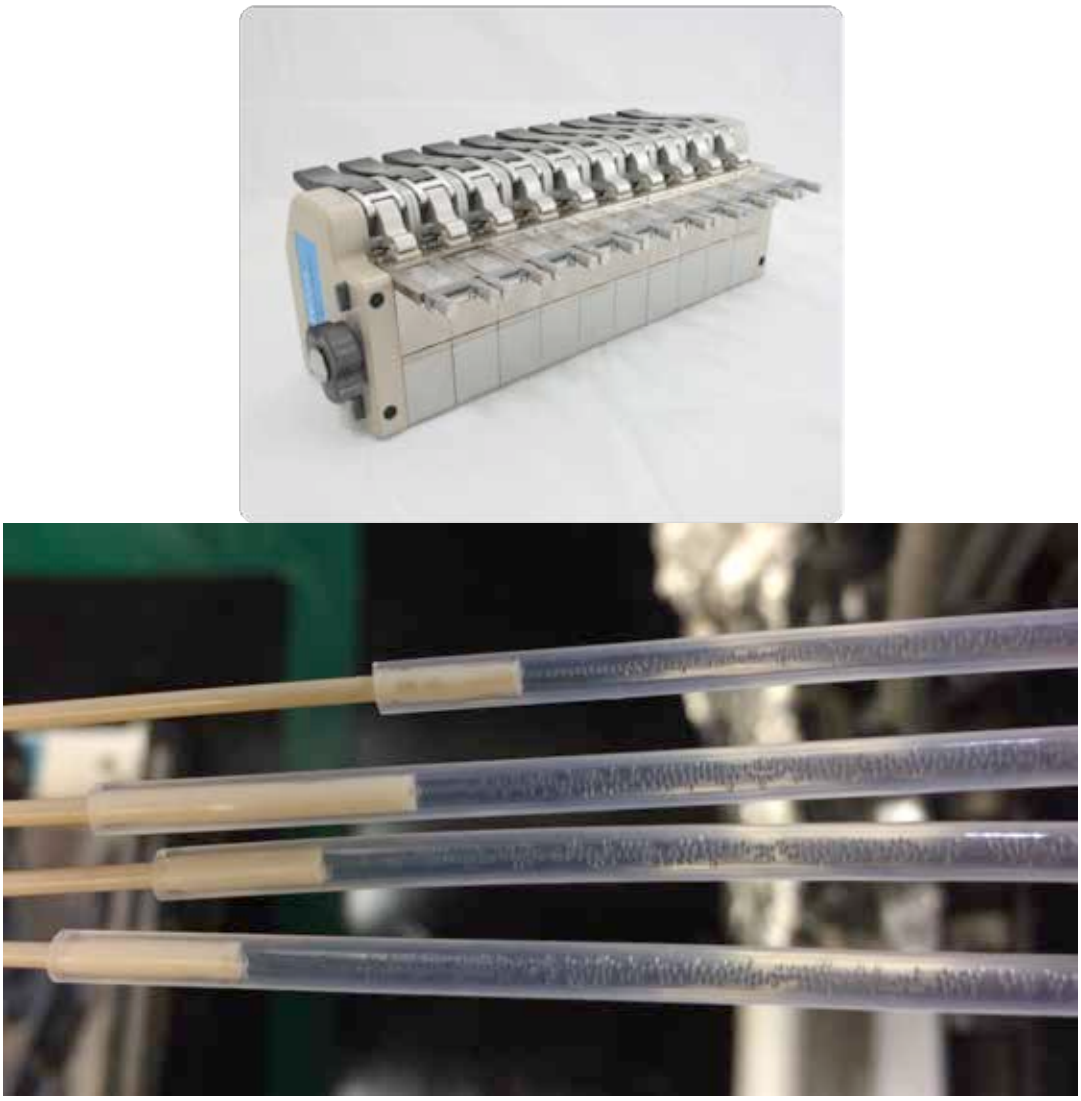

Figure 39: Top: Telos Parallel Microfluidic System® from Dolomite; Bottom: Four units running simultaneously from one chip, producing NDIL0309-Thiolene-Q microcapsules.

The parallelized microfluidic chip is also an option that we are considering for scale-up of the production of encapsulated NDIL0230. However, due to the challenges with producing NDIL0230 capsules (as described in Task 3.0), we have explored a rather different production strategy. This strategy, which is an in-air drop generator built at LLNL, is shown in **Figure 40**. The system pushes fluids out of a coaxial nozzle to form a core-shell fluid jet in air. As the nozzle is vibrated by an external device (a contact speaker in this case), we can control the jet breakup into drops. When a sinusoidal wave with a certain frequency (related to fluid properties, flow rate, and nozzle size) was applied, monodisperse drops were formed. Capsules will be produced when the drops are exposed to sufficient UV to crosslink the polymer shell. Even when the UV curing strategy was still under development, we demonstrated formation of double emulsions at

~250 g/hr. This method consumes no carrier fluid and potentially provides more control and repeatability of capsule formation than the parallel microfluidic approach.

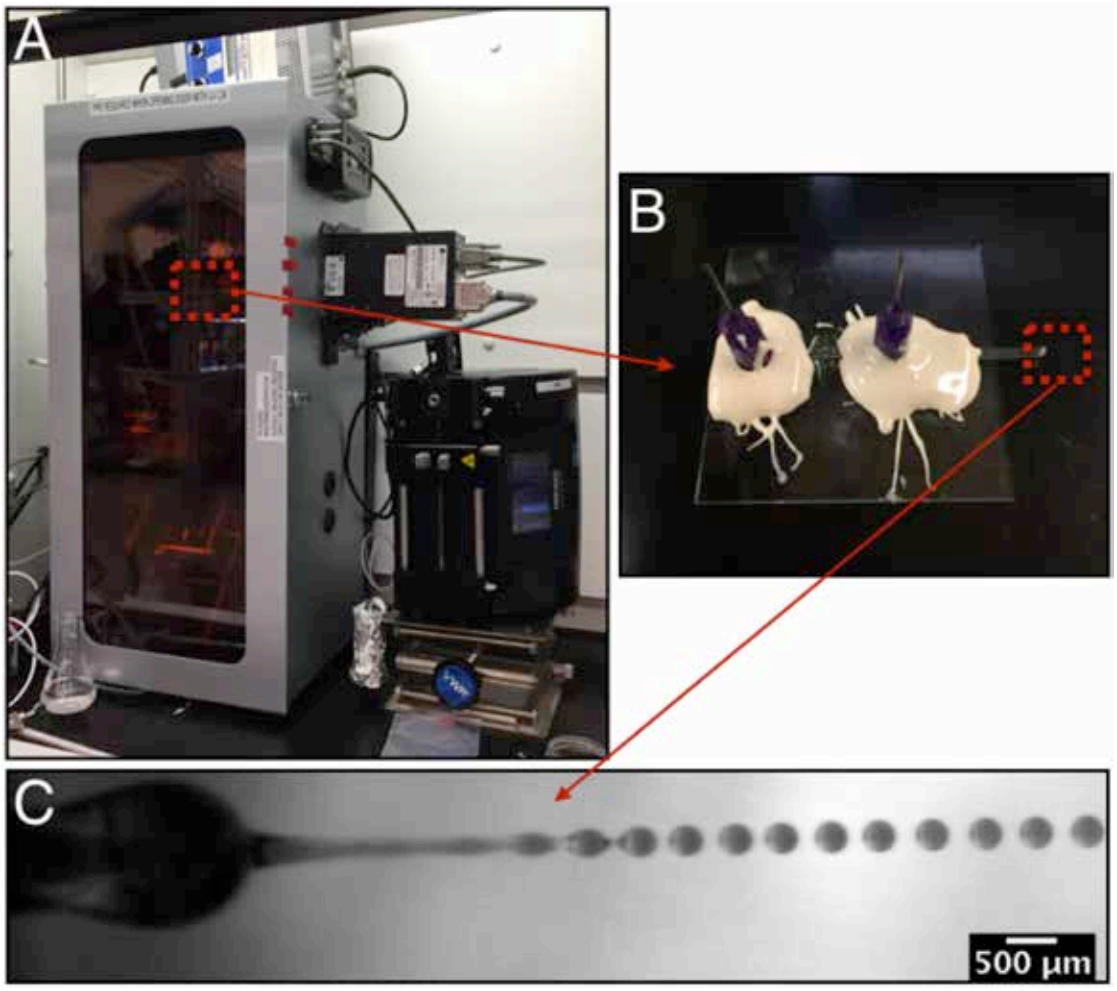

Figure 40: A) Overview of in-air drop generator box; **B)** A device example that was used to produce core – shell droplets; **C)** Production of carbonate SiTRIS droplets with in Air set-up, at a rate of 2000 drops/sec.

For identification of a scale-up method for the production of encapsulated NDIL0230, LLNL made a breakthrough in the In-air Drop Encapsulation Apparatus (IDEA). Shell material curing challenges were solved by using TPO-L as the initiator. This set-up will allow production of capsules about 60-100x faster than in our traditional device. One major challenge was the rupturing of capsules when they were collected. LLNL studied the various factors including UV power, UV "shadowing" by core, delayed curing, oxygen inhibition, size, shell thickness, shell strength, collection fluid surface tension, collection fluid agitation, air counter flow, and etc., and has found strategies to achieve consistent capsule production. In a brief trial, capsules containing neat NDIL0230 (100% neat IL) in Thiolene-Q (1:1 ratio) were successfully produced, at a rate of ~200 g/hr (see **Figure 41,** below). With the satisfactory demonstration of this alternate method for

producing NDIL0230 capsules, the IDEA apparatus has been selected as the scale-up method for encapsulating NDIL0230.

Figure 41: Photo of preliminary NDIL0230 (100% neat IL)-Thiolene-Q (TPO-L) capsules generated with IDEA system.

Subtask 10.2 – Produce ~1 kg of encapsulated ILs for the top two ILs/PCILs

As mentioned under Task 3, several large batches of NDIL0309 capsules have been prepared and sent to Notre Dame for testing and analysis (see **Figure 42**, below). The weight percent IL of each batch was labeled as the flow rates could vary in between batches. By the end of BP2, the total cumulative amount of as-produced NDIL0309 capsules exceeded 1 kg. This subtask is now complete for NDIL0309. LLNL continues to work on preparing NDIL0230 production with IDEA with the goal of producing 1 kg of NDIL0230 by 12/31/17.

The major challenge for production of NDIL0309 – Thiolene-Q was cleaning the chips. The microfluidic chip performance tends to degrade over time with usage. Different methods of cleaning the chips, as well as re-coating the surface were explored to extend the lifespan of the chips. Another challenge was the difficulty of measuring the IL% in the final product. This is because the pumps that process large volumes of chemicals are driven by pressure. There is no direct reading of the mass consumed per unit time. This problem was resolved by placing the pump on a balance so that we could monitor the mass change during operation.

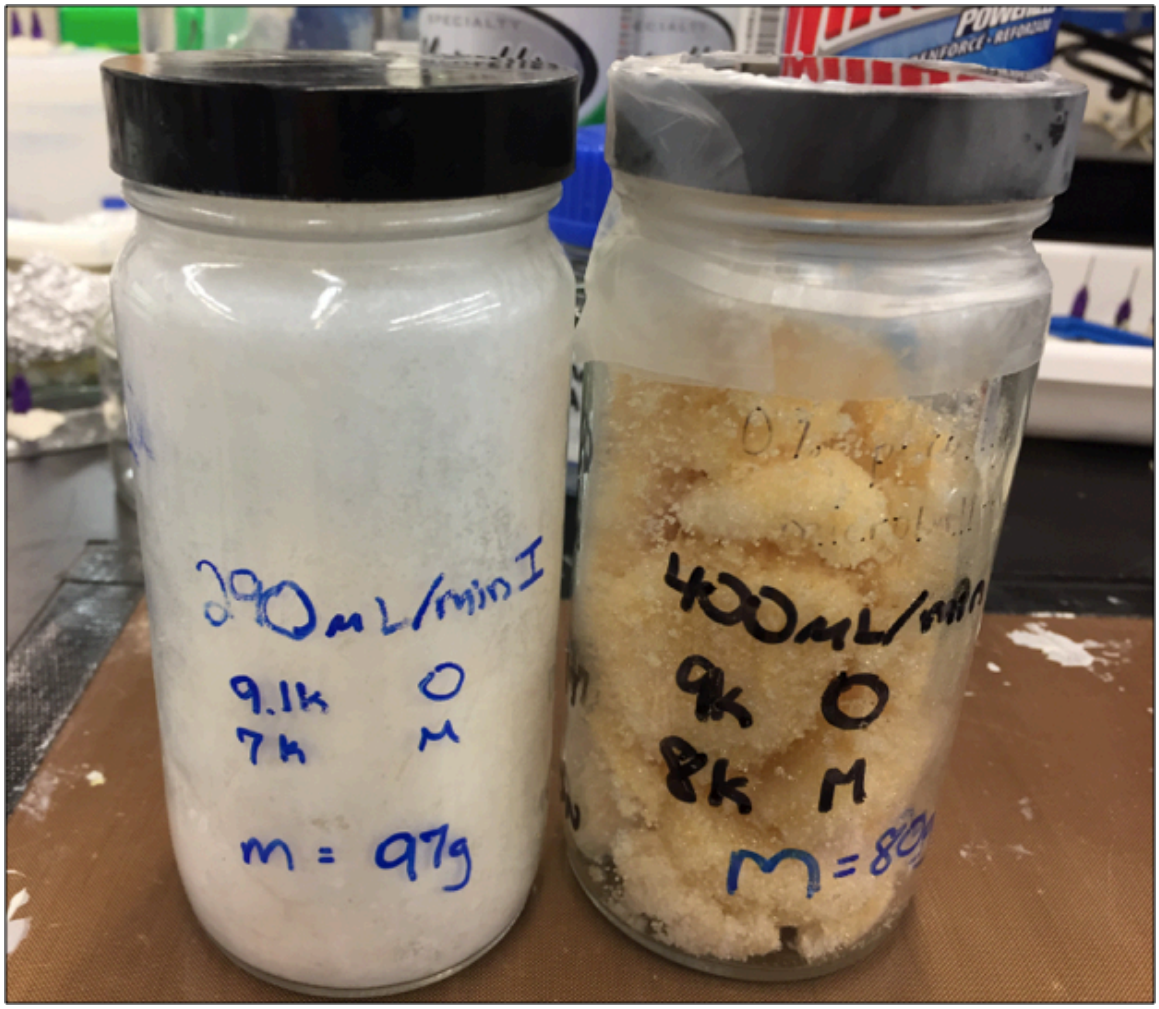

Figure 42: Photo of part of the NDIL0309 - ThioleneQ capsules produced and dried for Notre Dame's testing and analysis. The bottle on the left was coated with fume silica that helps fluidization test. The bottle on the right was uncoated and thus shows the yellow color of NDIL0309.

Task 11.0 – Construction and shake-down of laboratory scale unit for absorption and regeneration of IL microcapsules

The test system has been assembled and all components tested. Shake down runs for fluidization, pressure and temperature measurement, absorption and regeneration have been completed. Details are presented below.

Subtask 11.1 – Complete assembly of the test system, calibration and verification of all flow rate and pressure measurements, and operation of all analytical measurements

The next few photos show the flow set up without the columns and then with columns installed.

Figure 43: Skid mounted experiment rig inside a walk-in hood.

11.1.a. Columns

We have constructed the device to accommodate two columns at the same time. This reduces down time in some experimental situations and could be used to simultaneously do absorption and regeneration. The diameter of the columns can be varied as needed.

Figure 44: A 1-cm diameter column filled to a height of 3.5 cm with test particles, without gas flow.

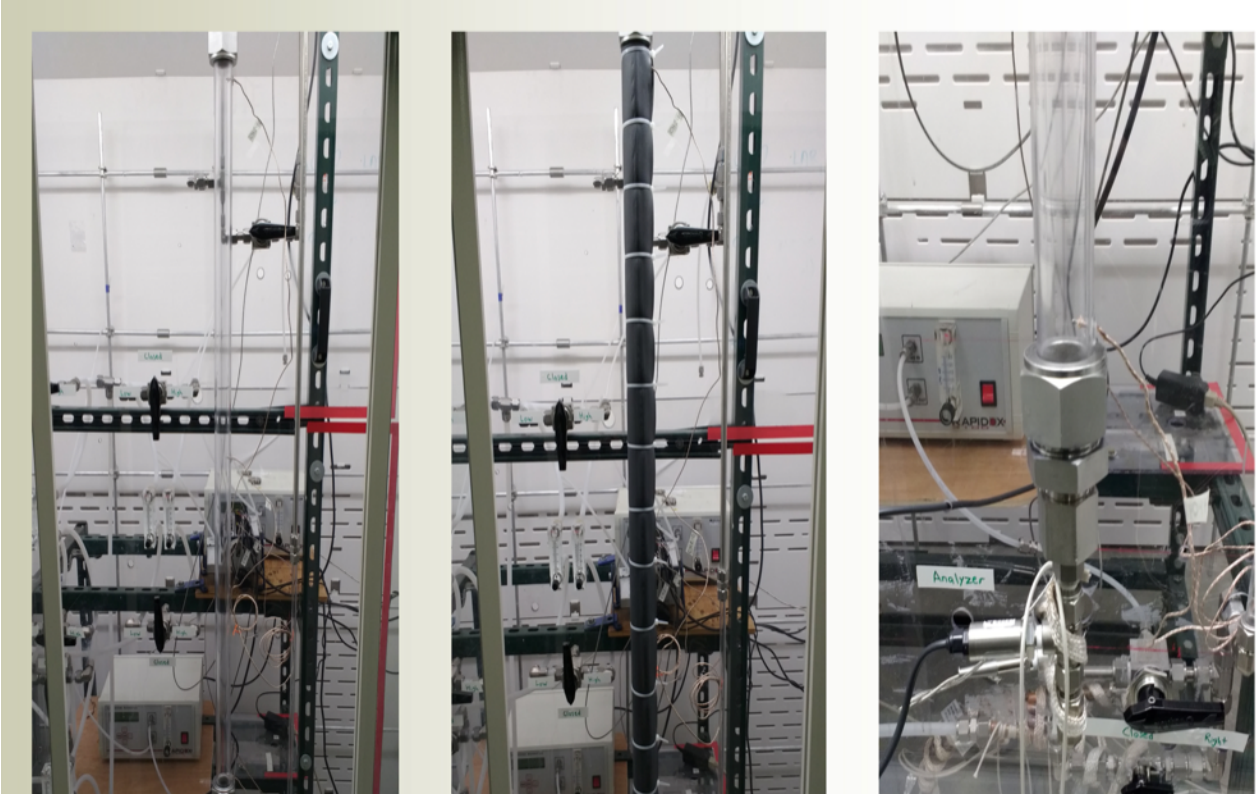

Figure 45: Photos of the test system with the 1.25-inch column installed

11.1.b. Gas feed system.

Three sets of rotameters are used to control gas feed to the column. Each feed can be varied from 0.5 to 100 l/min as needed by the experiment. One of the sets of rotameters is shown in Figure 13 (larger rotameters could be added if ever needed; valves and mounting holes have been added in case a 4th set or rotameters are needed). At present we use "house" nitrogen (from liquid N_2 tank boil-off) from a port inside the hood and carbon dioxide from tanks that are secured to a rack just outside the hood. Future experiments with SO_2 or NO_x will likewise utilize tanks outside of the hood.

Figure 46: One set of rotameters that cover up to 100 liter/min.

The concentration of CO_2 can be varied from 0 to 100% in the feed, although we have identified ~15% to 50% CO_2 in N_2 as the useful range. The low end mimics flue gas conditions and the higher values give increased sensitivity for more accurate mass transfer measurements.

11.1.c. CO_2 measurement.

The concentration of carbon dioxide in the inlet and exit gas is read using two Rapidox® gas analyzers, one of which is shown in **Figure 47**. This is accomplished by sending a small fraction of gas flow through the analyzers. For the inlet, the concentration is checked only periodically, since it is not changing, to eliminate any reduction of gas feed that would be lost through the analyzer.

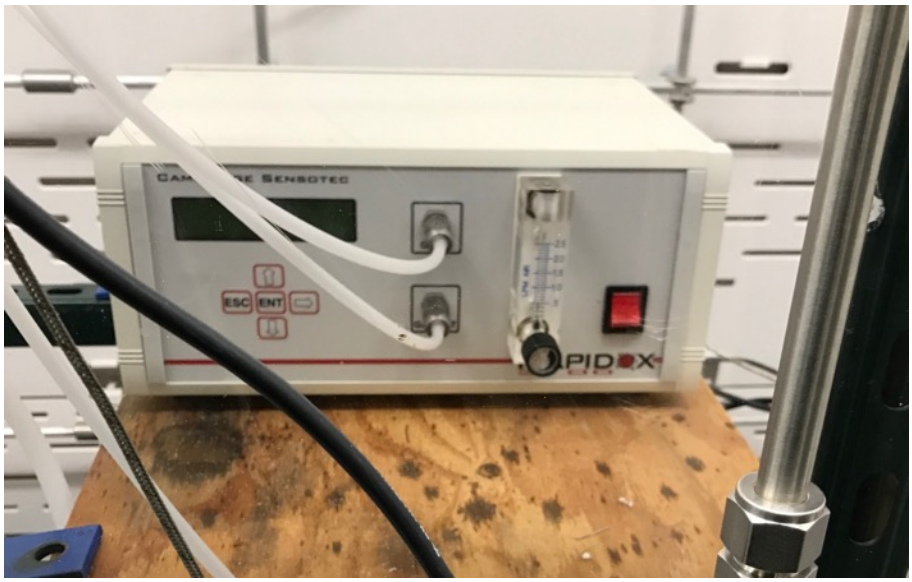

Figure 47: Rapidox ® Gas analyzer

The gas concentration was verified against the known inlet concentrations. We found that one of the analyzers was not performing well so we had it repaired by the manufacturer. The dynamical behavior was confirmed by changing the CO_2 gas feed rate. A series of step changes is shown in **Figure 48**. We see that below about 10% CO_2 the analyzer responds within a few seconds to the change. We see that for low concentrations, there is no need to account for the time lag. However, if we run absorption tests at higher inlet concentrations, we will need to correct the time response.

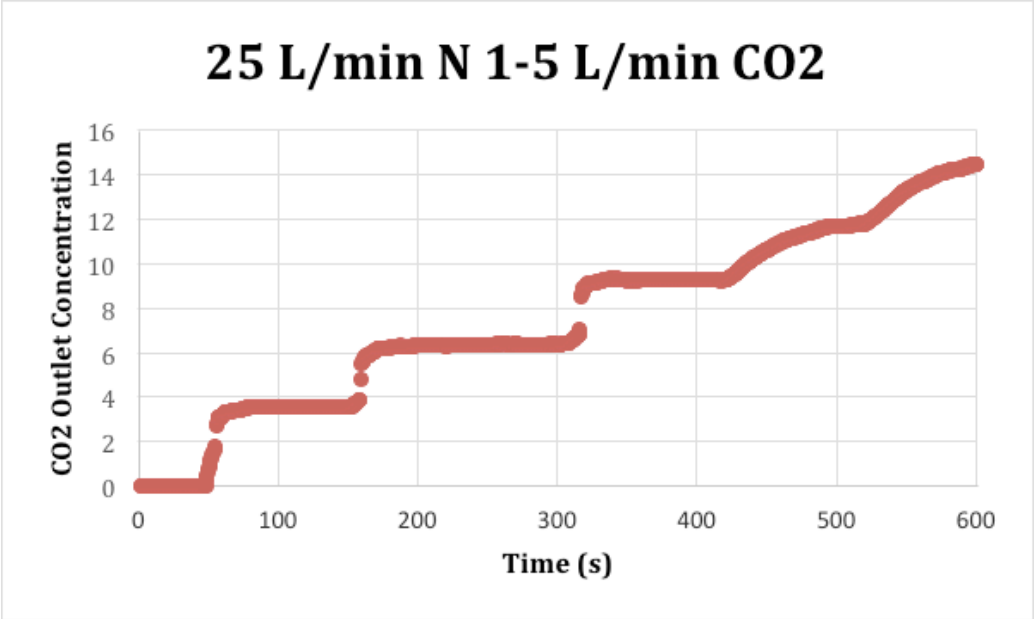

Figure 48: CO_2 outlet concentration response signal changes produced by step changes in CO_2 inlet concentration.

11.1.d. Pressure measurement

Pressure transducers with sensitivities of ~0.02 psi have been installed at the inlet and exit of the column, as shown in **Figure 49**. These provide continuous pressure values as a function of time, as shown in **Figure 50.**

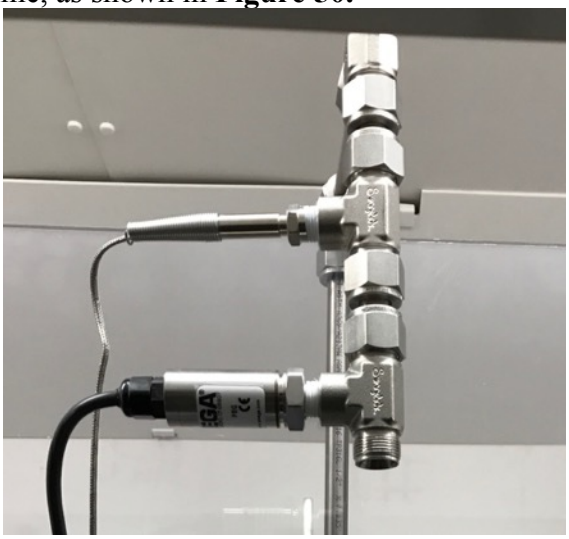

Figure 49: Thermocouple and pressure transducer at top column port.

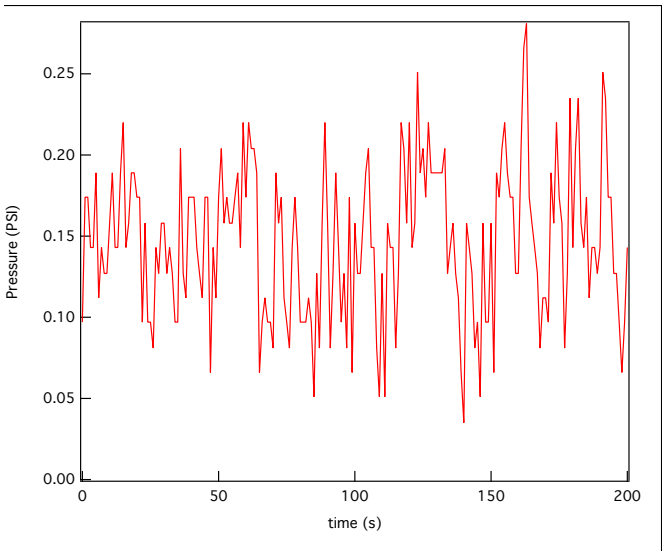

Figure 50: Pressure fluctuations during a fluidization test.

11.1.e. Temperature measurement.

Thermocouples have been installed at the inlet and exit plumbing (i.e., before and after the columns, which vary in height). For future experiments, we can insert thermocouples into the columns as necessary. As with pressure, we collect the temperature measurements continually in time. A photograph of the temperature and pressure interface module is shown in **Figure 51**.

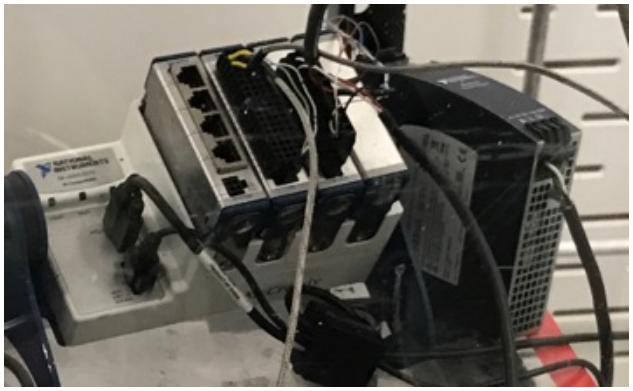

Figure 51: Interface module for thermocouples and pressure transducers.

11.1.f. Gas heater for regeneration

Figure 52 shows the heater that is used to regenerate the capsules. It is a gas loop wrapped with heating tape. We can control the heating rate and hence the temperature of the gas that is used for regeneration. Our initial tests indicated that we needed more length and surface area, which is now installed.

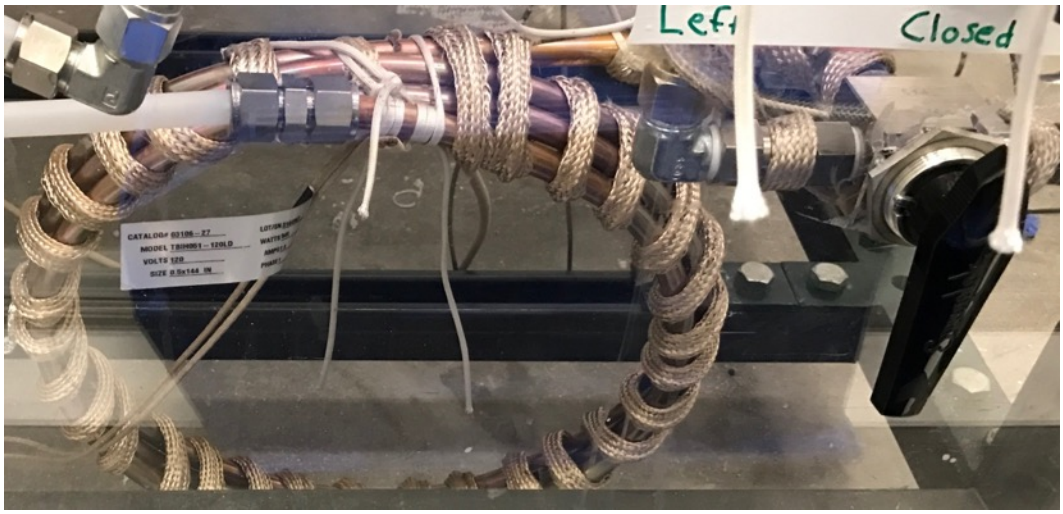

Figure 52: Preheater assembly – inlet loop.

In addition, we insulated the column, as shown here in **Figure 53**. However, since viewing the experiments could occasionally be convenient, we constructed the system so that this new black insulation can be removed.

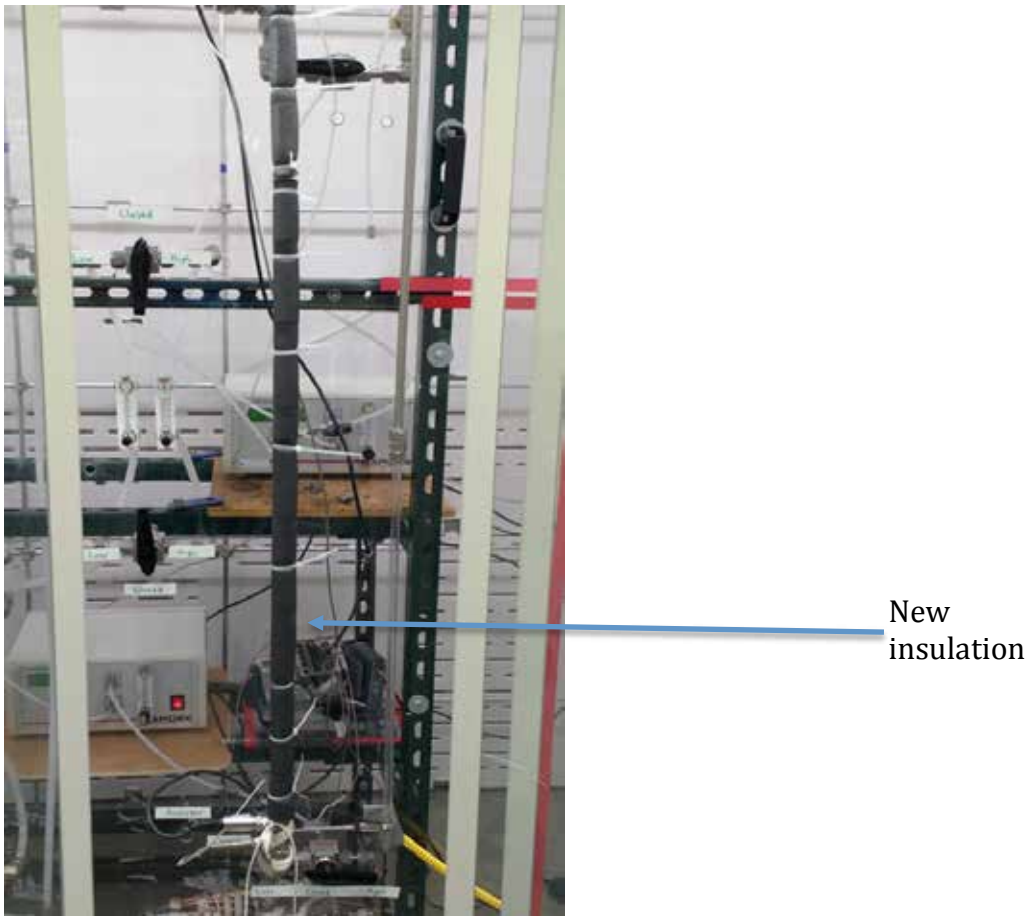

Figure 53: Test rig with new insulation (as shown)

A test of the heater and the thermocouples is shown in **Figure 54**. The exit temperature remained close to room temperature, which motivated the need for the insulation that was added to the column.

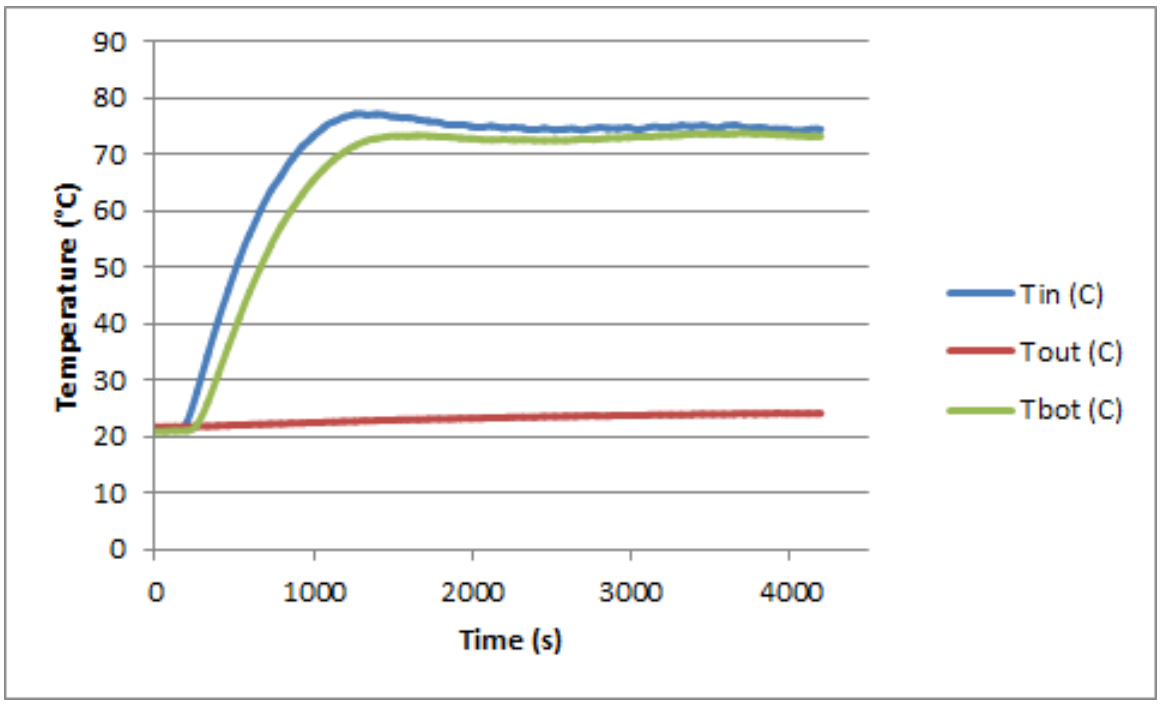

Figure 54: Temperature response curves reflecting step changes in feed heater temperature.

We have also checked our ability to choose the temperature of the largest column as shown in **Figure 55**.

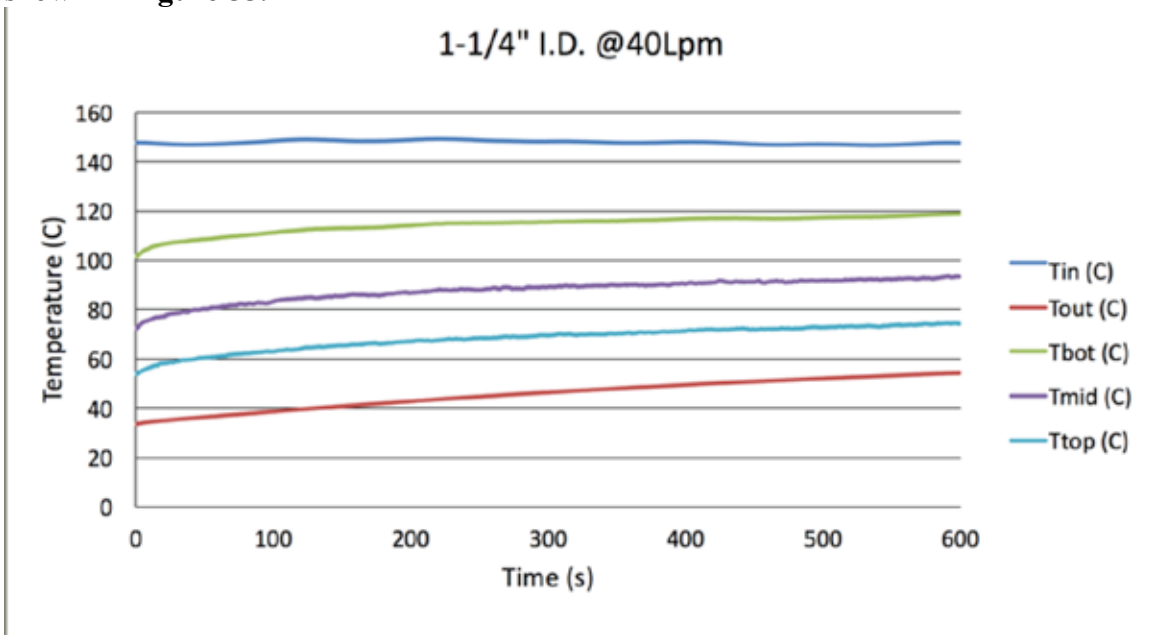

Figure 55: Temperature versus time in the fluidized bed during a temperature ramp-up

Subtask 11.2 – "Cold Flow" experimental runs on inert particles

11.2.a. Examination of fluidization

We used 300 μm polyethylene spheres as the inert particles. These fluidize very easily. The photographs below (**Figures 56a and 56b**) are snapshots of video clips that can be made available.

Figure 56a: Pictures of fluidization of polyethylene spheres at gas flow rates of 1.0, 2.0 and 3.0 l/min.

Figure 56b: Pictures of fluidization of polyethylene spheres at gas flow rates of 4.0, 4.7 and 5.0 l/min.

A plot of the height of the bed as a function of flow rate is shown in **Figure 57**. The linear increase with flow rate up about 2.0 l/min is indicative of a slowly expanding bed. Above this value the bed is fully fluidized. As the gas flow is increased past about 3.0 l/min, particles are beginning to be lost out of the top.

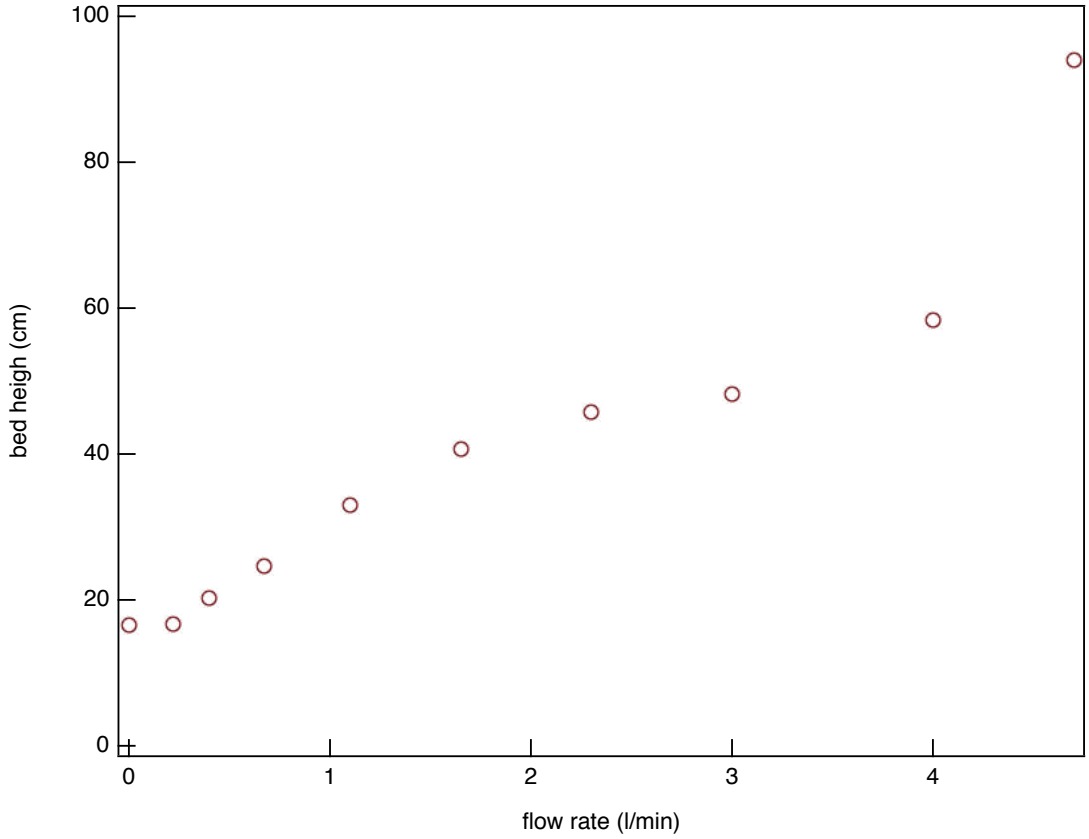

Figure 57: The expansion of the packed particles into a fluidized bed

11.2.b. Pressure drop

The pressure drop depends on the flow rate and the quantity of particles in the column. As seen in the figure below (see **Figure 58**) for measurements at the start of a fluidization test, the pressure difference is about 0.13 psi. The pressure fluctuations that result from irregularities in the flow associated with fluidization are also 0.1 psi, with a time scale of 2-3 s.

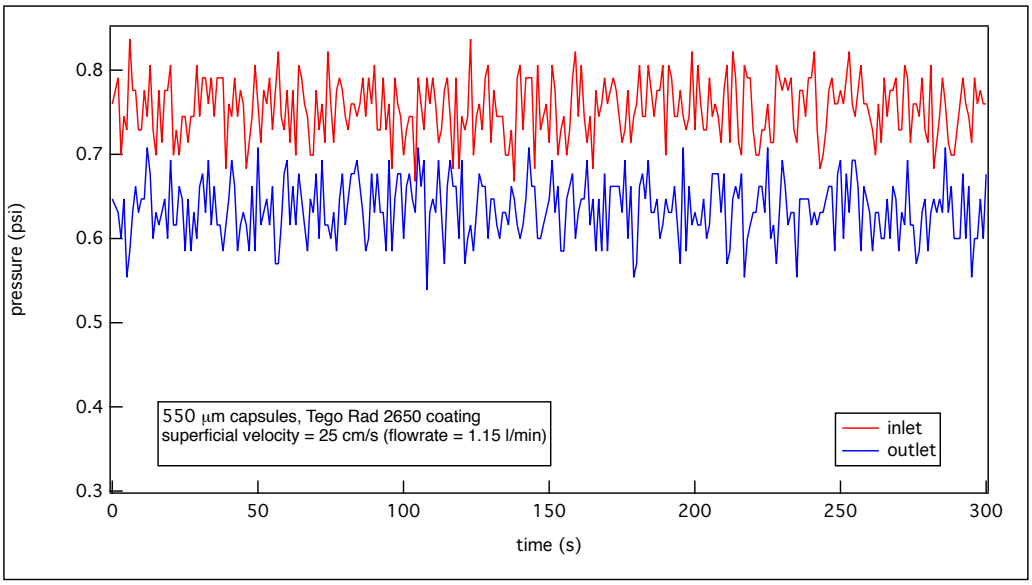

Figure 58: Pressure fluctuations during a fluidization run.

We have also tested the flow/fluidization behavior for the capsules in the 1.25 in column. A series of photos are shown here. The accompanying video can be provided.

A close viewing of the photos below (**Figures 59a, 59b, and 59c**) shows that at a flow rate of 4.0 and 5.0 LPM, the bed is "slugging". The alternating lighter and darker regions match with higher and lower concentrations of capsules. The "slugs" travel upward in the bed, but are not fixed portions of solids. A lot of capsules are being shed at the bottom and new ones collected at the top of the moving slugs.

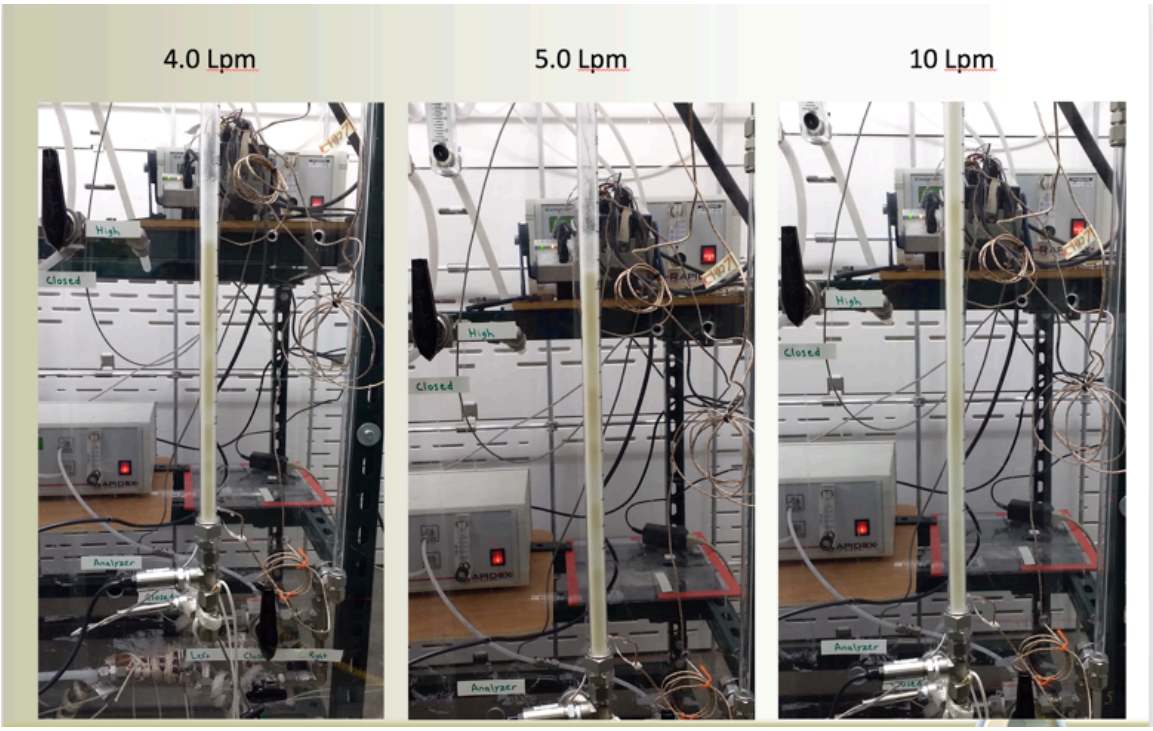

Figures 59a, 59b, and 59c: Series of photos of the large column at different gas flow rates showing bed "slugging."

The pressure drop for the capsules in the large column is seen in the graph below, **Figure 60**. The circles are the bed height, which is fixed until about 2 Lpm when the bed begins to expand. The pressure drop, (diamonds), jumps to a high value (0.46 psi) until the bed begins to fluidize and then it drops and remains almost constant with increased flow rate at about 0.25 psi. The sharp increase occurs because the capsules are slightly "sticky" and it takes some "tapping" on the outside of the column and an increased flow rate, to expand from a packed bed where they are touching, to a fluidized bed.

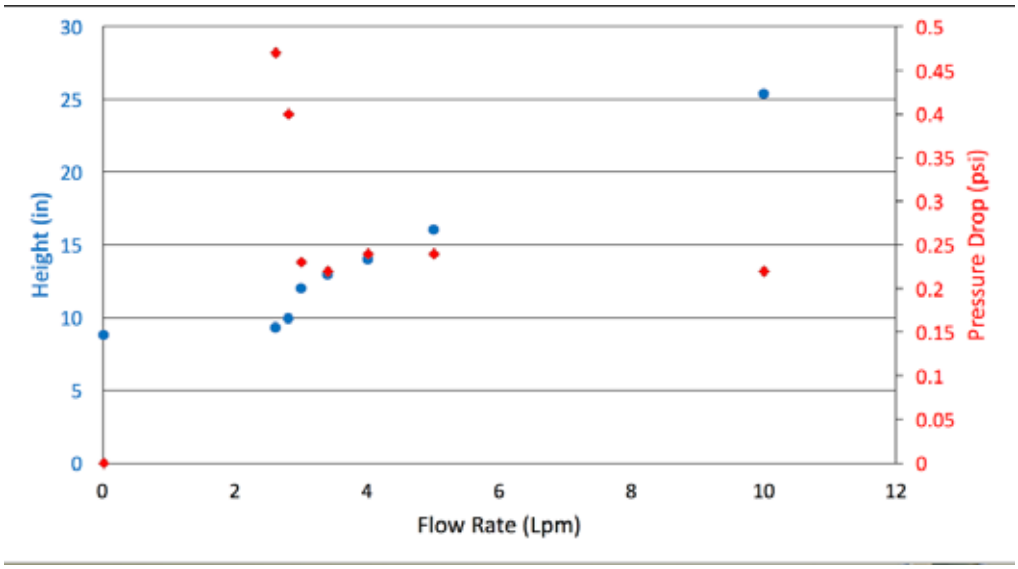

Figure 60: Fluidized bed height (i.e., expanded height) and pressure drop across the fluid bed as a function of gas flow rate.

Task 12.0 –Modeling

We have compared measured mass transfer flux in the fluidized and packed beds to predictions from our rate-based model, refining the model to better represent the actual process. We have also incorporated optimization and sensitivity capabilities in the rate-based model for the fluidized bed and used those capabilities to recommend improvements that can be made to the microcapsules.

Subtask 12.1 – Refinement of rate-based models

Working with the experimental group (task 7.1) we have compared the measured mass transfer flux in a fluidized bed of microcapsules with the predicted mass transfer flux from our rate-based fluidized bed model. The microcapsules contain the phase-change ionic liquid NDIL0309 and have a diameter of 560 microns. The fluidized bed was operated at a temperature of 343.15 K. The results are shown in **Table 3**.

The model provides quite good agreement with the experimental measurement, being only about 30% lower. Thus, we believe that the model provides a good conservative estimate of the mass transfer flux. The model indicates that most of the resistance to mass transfer occurs in the liquid inside the microcapsules. Two noteworthy uncertainties in the model are 1) the liquid viscosity, which in this case, since NDIL0309 is a PCIL, is the viscosity of the IL-CO_2 complex, and 2) the reaction rate constant. Neither of these two quantities has been directly measured, so in the model we have used typical values from other AHA ILs. These parameters could be tuned to make the model more closely match experimental data.

We also obtained data for the measured mass transfer fluxes for Thiolene-Q encapsulated NDIL0309 microcapsules in a packed bed, and did a comparison to our corresponding model. As shown in **Table 7**, in this case the model also provides a good estimate, but an overestimate. However, in discussion with the experimental group, it was found that a visual observation of the packed bed experiment showed that not all of the microcapsules were contacted by the flowing gas. Thus not all of the microcapsule area was used. To account for this, we have added an empirical effective area factor to the microcapsule packed bed model, with an estimated value based on the visual observation of 0.5. This makes the fluidized bed and packed bed models more consistent, with both providing a small underestimate of the experimental mass transfer flux.

Table 7: Comparison of measured and predicted mass transfer fluxes.

	Measured mass transfer flux (mol/(m^2 s)	Predicted mass transfer flux (mol/(m^2 s)
Fluidized Bed	4.84×10^{-4}	3.33×10^{-4}
Packed Bed	1.66×10^{-4}	2.40×10^{-4}
Packed Bed with Effective Area Factor	1.66×10^{-4}	1.20×10^{-4}

We have also incorporated optimization and sensitivity analysis capabilities into the fluidized bed mode. Thus, we have performed various sensitivity and optimization studies of interest. Two examples are given here.

The first example shows the sensitivity of process performance (parasitic energy and required fluidized-bed absorber size) to changes in the solvent viscosity. This is of interest since LLNL's recent work has considered increasing the IL fluid viscosity with added glycerol to improve encapsulation performance. Results are shown in **Figure 61**, which indicates that performance is relatively insensitive to modest increases in viscosity. This shows results for one specific set of IL physical properties and process conditions; results are similar when other typical values are used.

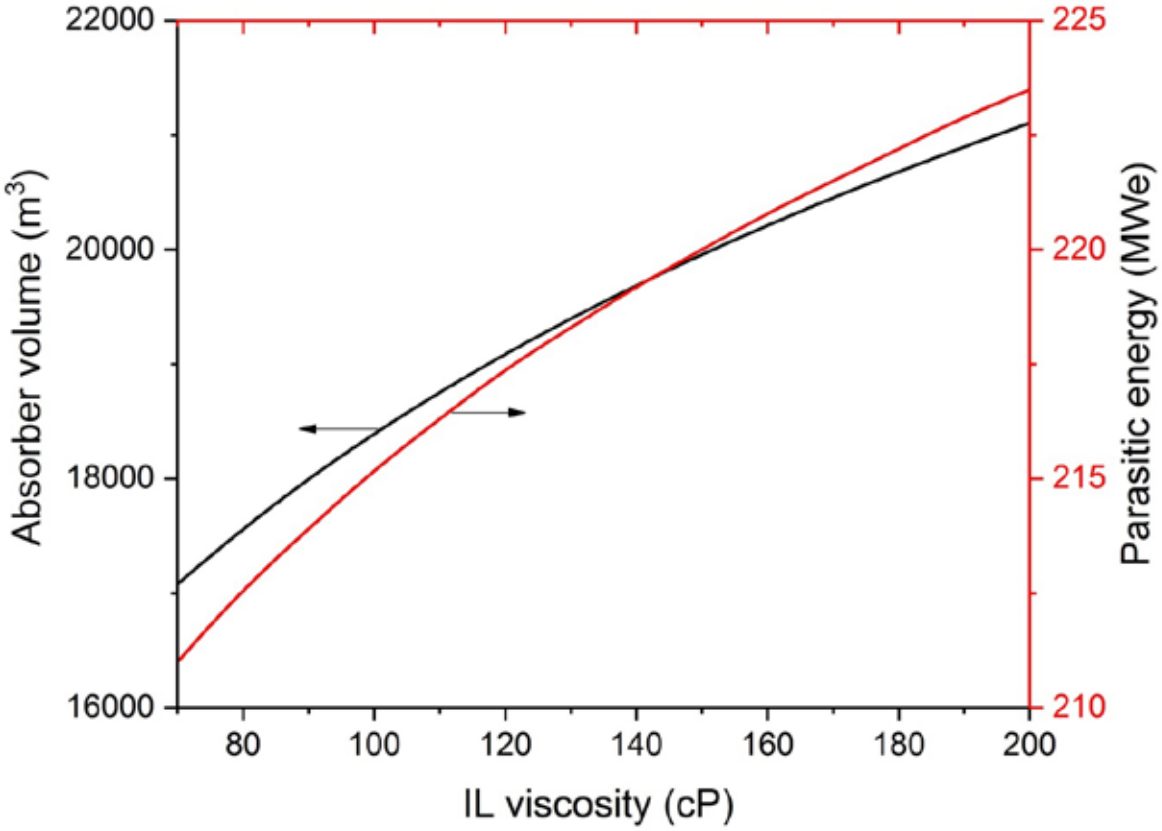

Figure 61: Sensitivity of the parasitic energy (MWe) and absorber volume (m^3) at different solvent viscosity vales (70 – 200 cP). Operating conditions: absorber temperature = 293.15K, stripper temperature = 413.15 K, absorber pressure = 1 bar, stripper pressure =1 bar. IL properties: chemical absorption enthalpy = −45 kJ/mol, chemical absorption entropy =−122 J/(mol K). Microcapsule diameter = 200 microns.

In the situation shown in **Figure 61**, the performance objectives both move in the same direction as the sensitivity parameter of interest is varied. However, this is often not the case, as the parasitic energy and absorber volume (a proxy for capital cost) may be competing objectives for which there are tradeoffs. For these cases the use of Pareto analysis may be useful. For example, **Figure 62** shows the situation when the stripper temperature Ts is varied, which shows a type of Pareto curve. In the part of the curve with a positive slope, both objectives are increasing, indicating a clearly undesirable range of operation. But in the part of the curve with a negative slope, there is a tradeoff between the two objectives. The decision maker can then determine how to weight the competing objectives, perhaps using additional economic analysis. The situation in **Figure 62** is that using a higher Ts leads to a leaner sorbent flowing back to the fluidized bed, which increases the overall absorption rate and reduces the reactor volume. But the higher Ts also requires that hotter and thus more valuable steam be extracted from the power plant steam cycle. This effect is reduced as Ts is lowered, but the overall parasitic

energy is reduced only up to the point where the increased blower energy required by the larger absorber begins to predominate.

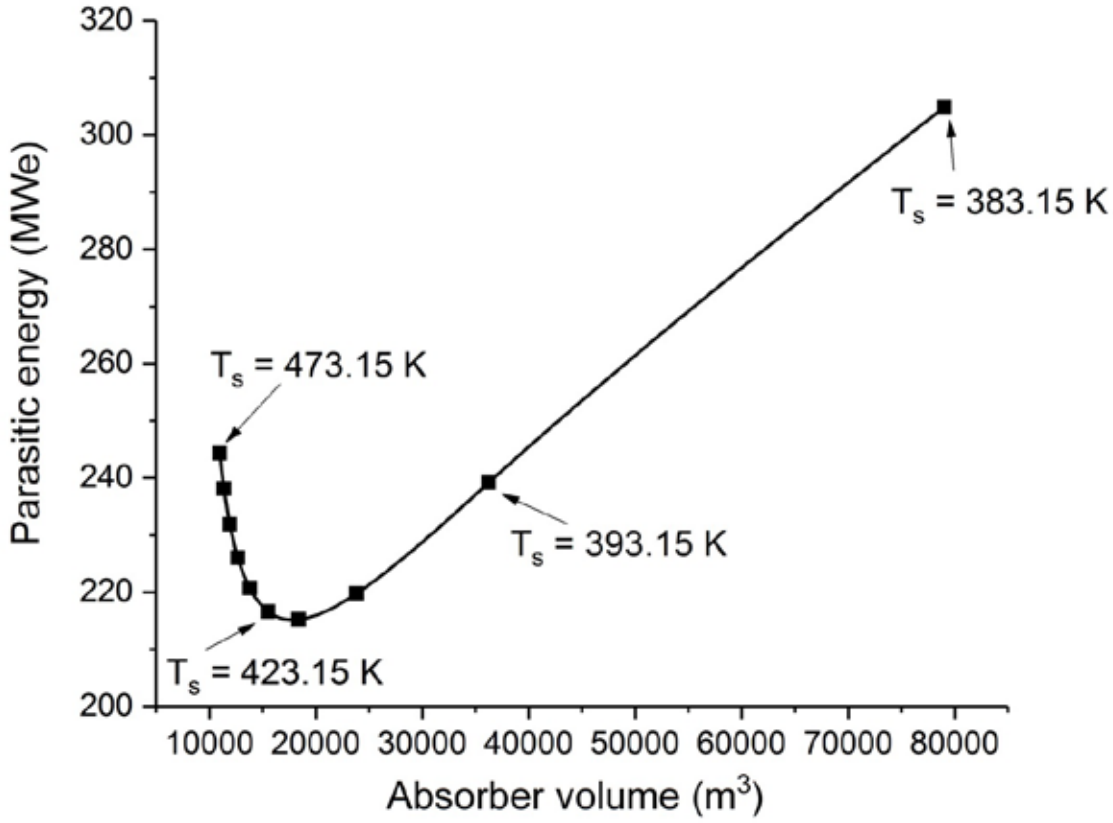

Figure 62: Sensitivity of the parasitic energy (MWe) and absorber volume (m^3) with respect to stripper temperature Ts. Operating conditions: absorber temperature = 293.15K, absorber pressure = 1 bar, stripper pressure =1 bar. IL properties: chemical absorption enthalpy = −45 kJ/mol, chemical absorption entropy = ~122 J/(mol K), viscosity 100 cP. Microcapsule diameter = 200 microns.

Subtask 12.2 – Use of rate-based models to identify targets for microcapsule properties

We have used the rate-based fluidized bed model to conduct optimization and sensitivity analysis of microcapsule properties. The model trends follow our qualitative expectations, but provide quantitative measures of the sensitivity of the process to microcapsule properties of interest. Two examples are given here. **Figure 63** shows how the total required microcapsule volume, which is directly related to the absorber volume and thus the process capital cost, varies with the weight percentage of IL in the microcapsules. This also has a direct impact on the microcapsule shell thickness, as

shown in **Figure 10**, but the reduction in required volume is due almost entirely to the increased amount of IL per microcapsule rather than the thinner shell.

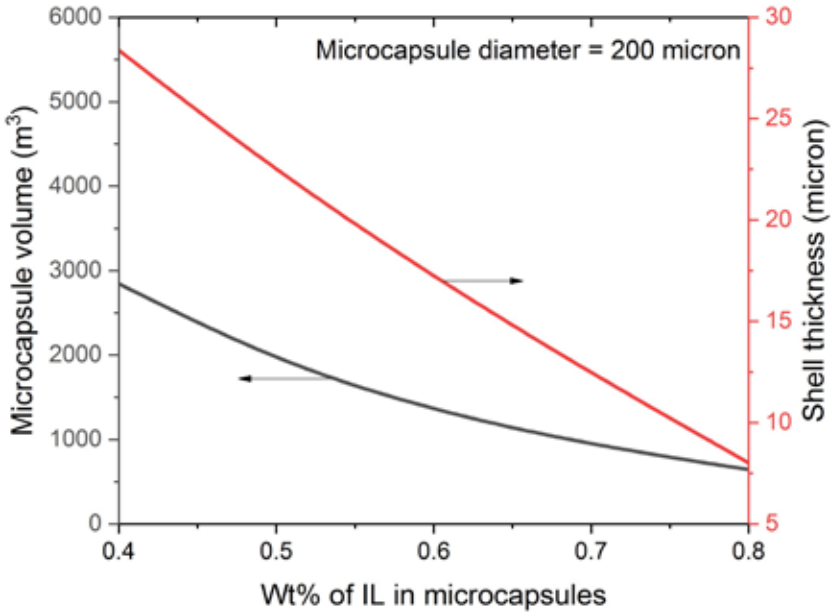

Figure 63: Sensitivity of total required microcapsule volume and microcapsule shell thickness to changes in weight percent of IL in microcapsules. Absorber temperature = 303.15 K, stripper temperature = 473.15 K, absorber pressure = 1 bar, stripper pressure = 1 bar, heat of chemical absorption = −50 kJ/mol, entropy of chemical absorption = −130 J/(mol K), IL viscosity = 100 cP, shell permeability = 3300 barrers, and microcapsule diameter = 200 micron.

Figure 64 shows the relationship between the total required microcapsule volume and the microcapsule diameter, for several values of the weight percent IL. It is seen that significant improvements in required volume, especially at lower weight percent IL can be achieved by reducing the microcapsule diameter. This is due to increasing the surface area per unit volume of microcapsules. We recommend that a somewhat smaller microcapsule diameter than that currently being used should be targeted.

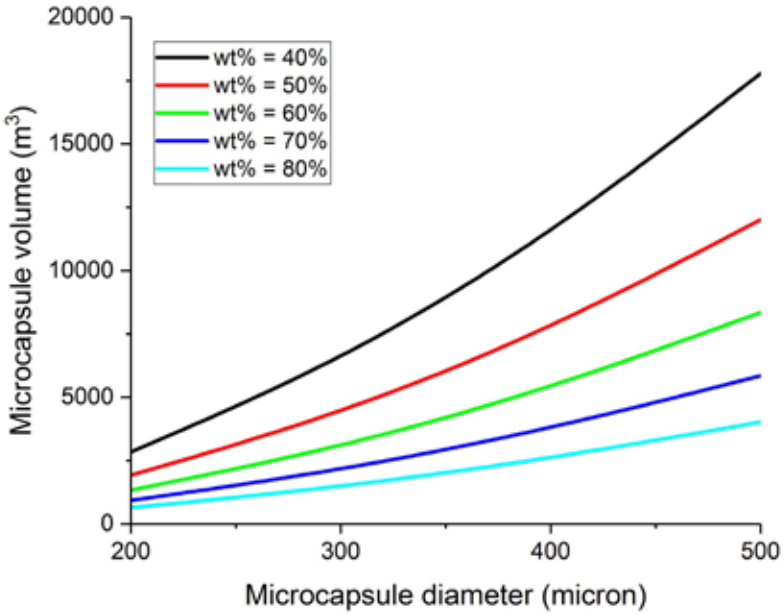

Figure 64: Sensitivity of total required microcapsule volume and microcapsule shell thickness to changes in microcapsule diameter. Absorber temperature = 303.15 K, stripper temperature = 473.15 K, absorber pressure = 1 bar, stripper pressure = 1 bar, heat of chemical absorption = −50 kJ/mol, entropy of chemical absorption = −130 J/(mol K), IL viscosity = 100 cP, and shell permeability = 3300 barrers.

Task 13.0 – Initial testing of silicone IL microcapsules in fluidized bed or packed bed absorber with CO_2/N_2 mixture

Subtask 13.1 – CO_2 capture experiments in fluidized bed

The essential processes necessary for effectively operating the largest absorption column, which has a diameter of 3.4 cm, as described below.

Fluidization behavior: **Figure 65** shows a fluidization experiment using about 66 g of capsules in the 3.4 cm column. The height of the bed is seen to expand as expected with increasing gas flow rate and reaches a nominally stable value at about 45 cm. The pressure drop across the bed increased with increasing gas flow rate, as expected. Visual observations indicated that the bed was largely well fluidized, although there was probably a small quantity of capsules in the bottom of the column that were not completely fluidized. We would have liked to have continued to higher flowrates, but the nitrogen supply to the lab that day was limited for some reason. We will repeat this experiment in the future with larger quantities of capsules, but we don't expect any problems with the fluid mechanics of the column.

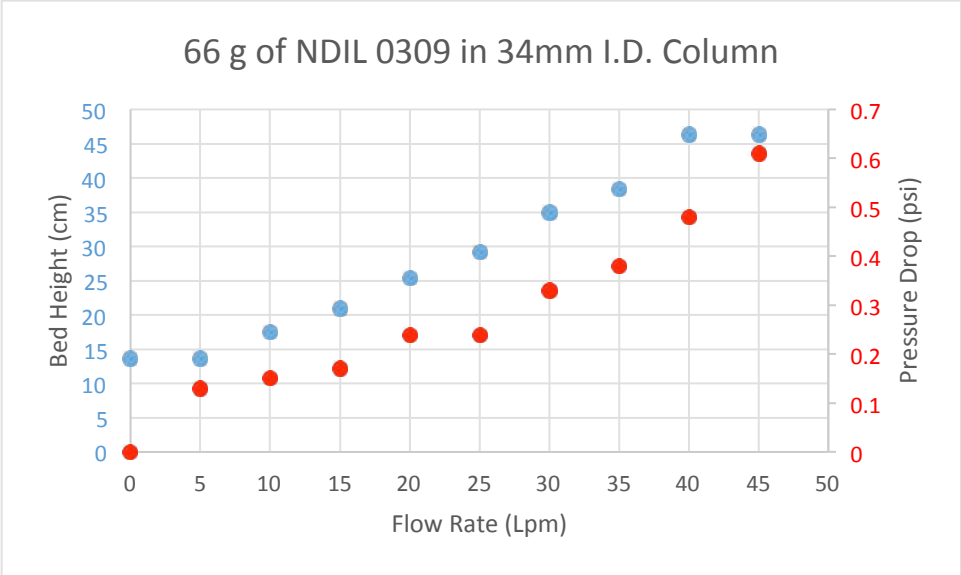

Figure 65: Fluid bed performance (bed height and pressure drop) of NDIL0309 capsules in 34 mm ID column (red data points = static bed; blue data points = fluidized bed)

Subtask 13.1/13.2 – CO_2 capture/desorption experiments in fluidized bed

Absorption/desorption runs

Table 8 shows a series of absorption runs for NDIL0309 in Thiolene-Q. **Table 9** shows additional set of runs. These were test runs for absorption/desorption in the 3.4 cm column.

Table 8: Results of nine cycles of CO_2 absorption and regeneration for NDIL0309 samples in the fluidized bed unit.

Cycle	Mass (g)	Ending Mass (g)	Total Flow (Lpm)	Absorb Temp (°C)	Regen Temp (°C)	Pco2 (bar)	L CO2	CO2/IL (mol ratio)
1	63.526	48.45	29.5	60	110	0.038	1.01	0.41
2	48.45	--	24.7	60	110	0.042	0.5	0.27
3	48.45	--	29.5	60	110	0.044	0.36	0.19
4	48.45	32.455	29.3	60	110	0.035	0.26	0.2
5	32.455	--	19.8	70	120	0.058	0.59	0.47
7	32.455	--	29.1	70	120	0.041	0.38	0.3
8	32.455	--	30	70	120	0.088	0.42	0.33
9	32.455	--	35.6	70	120	0.076	0.46	0.36

Table 9: Results for a second series of eight cycles of CO_2 absorption and regeneration for NDIL0309 samples in the fluidized bed unit.

Cycle	Mass (g)	Total Flow (Lpm)	Absorb Temp (°C)	Regen Temp (°C)	Regen Time (hr)	Regen Flow (Lpm)	Pco2 (bar)	L CO2	CO2/IL
10	59.4	25.4	70	120	3	25	0.051	1.9	0.82
11	59.4	25.2	70	120	4	30	0.047	0.56	0.24
12	59.4	24.9	70	120	3.5	25	0.055	0.35	0.15
13	59.4	25	70	120	3	35	0.056	0.23	0.1
14	59.4	24.9	70	120	3	45	0.054	0.45	0.19
15	59.4	25.4	70	120	5	45	0.051	0.57	0.25
16	59.4	25.4	70	130	3	30	0.047	0.54	0.23
*17	59.4	25	70	130			0.064	0.92	0.4

*Regeneration before this run was using pure CO_2

Over the course of these runs we examined the absorption and regeneration temperatures and times, a range of gas flow rates and inlet concentration. The capsules used for these experiments were from various batches and were not from a single uniform production run. We found that it is essential to absorb at or above 60°C to make sure that the PCIL will become a liquid, and regenerate at or above 120°C. These runs demonstrate that the general functions of absorption/desorption are occurring in the system but the small amount of capsules and lack of their uniformity, contribute to rather irregular measurements of uptake on specific runs.

Concentration traces from recent set of runs with a new batch of capsules, taken from a larger "production" run from LLNL is shown in **Figure 66**.

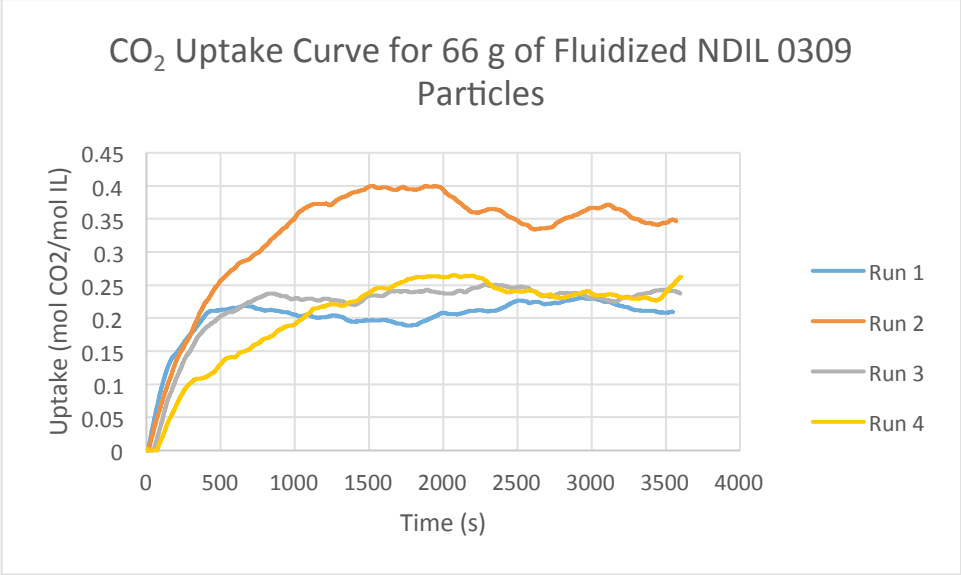

Figure 66: CO_2 Concentration vs. time on stream for a series of four runs using NDIL0309 capsules. Concentration profiles show the consistency of breakthrough times of CO_2 in the fluidized bed.

The final values for CO_2/IL mole ratio, which is about 0.25 mole CO_2/mole IL are shown more clearly in **Figure 67**.

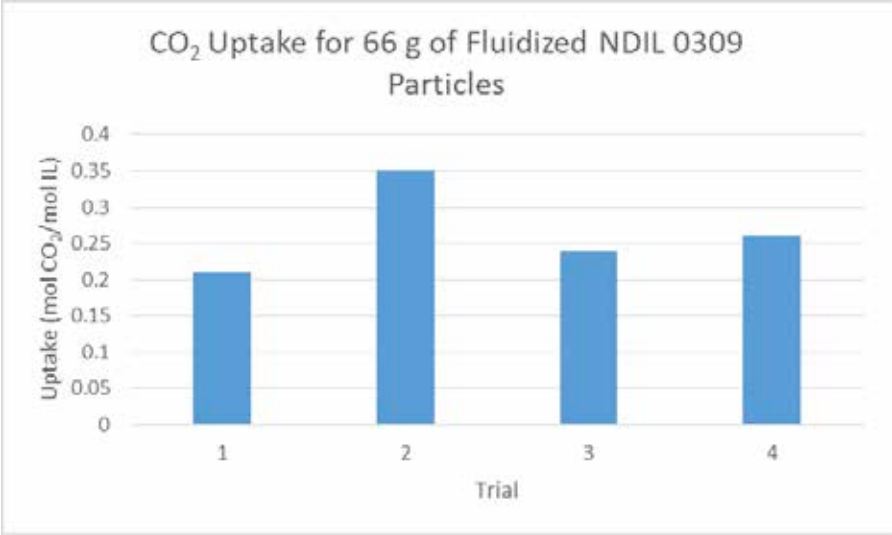

Figure 67: Final uptake values, expressed as mol CO_2/mol IL for the series of four fluidized bed runs with NDIL0309 capsules.

With the exception of Run 2, during which we think that we had an analyzer problem (since fixed), the uptake of CO_2 is consistent at about 0.25 mole CO_2/mole IL. This is a great improvement over the initial runs shown above where the uptake value varies rather considerably and randomly from run to run.

Figure 68 shows these uptake values plotted on the equilibrium curves for NDIL0309 and CO_2. Note that the 0.25 mole CO_2/mole IL equilibrium uptake is about 50% of the expected value.

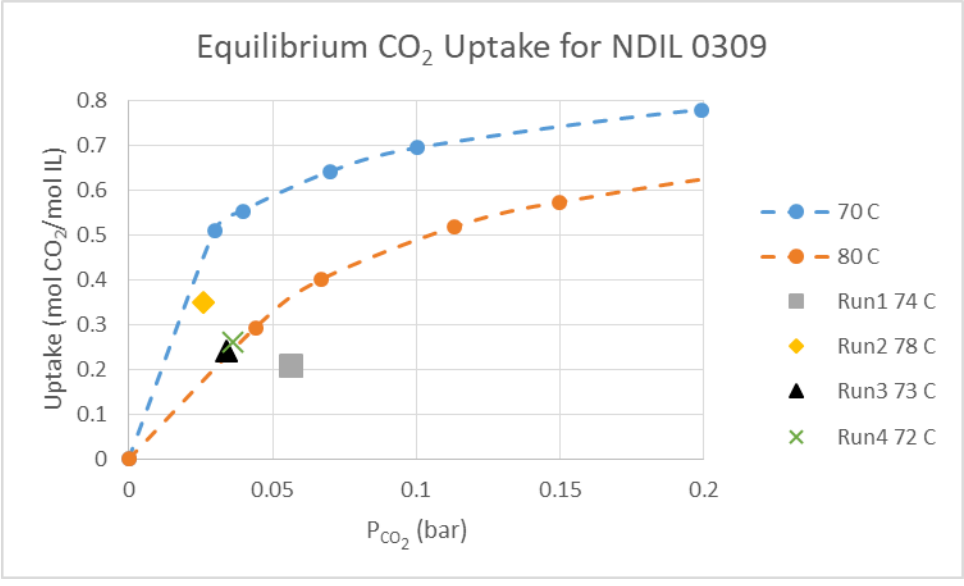

Figure 68: Uptake values plotted on the equilibrium curves for NDIL0309 and CO_2

The calculated mass transfer coefficients and CO_2 partial pressures for these runs are given below in **Table 10**.

Table 10: Computed mass transfer coefficients (k, cm/sec) for CO_2 uptake by NDIL0309 capsules for each of the four fluidized bed runs.

Run	Pco2 (bar)	Mol Ratio	k (cm/s)
1	0.056	0.21	5.19E-05
2	0.026	0.35	1.65E-05
3	0.034	0.24	3.24E-05
4	0.036	0.26	2.87E-05

While the mass transfer coefficients are in the same range as we measured in the smaller columns, the partial pressures of CO_2 that we used for the runs in this larger column are lower than for the previous experiments in smaller columns by a factor of as much as 5. While in principle the CO_2 concentration really should not matter, , as we are comparing the uptake to equilibrium values at the same CO_2 partial pressure, perhaps this is the reason for the lower ratios. The lower CO_2 values arise in our system as a result of several factors as the nitrogen is supplied as a house utility and we use cylinders of CO_2. Each of these feeds has a separate metering system. In any case, we will modify the gas feed system to get partial pressures of CO_2 that match values that were achieved in our previous experiments with the smaller column. Once this is done we expect to be able to achieve the previous loadings that were close to the equilibrium values.

We received a large batch of capsules from LLNL in September in time to try one run with about 170 g of capsules, which is about 3 times the mass as any previous run. While it cannot be seen in the uptake (since we showed earlier that good fluidization is not essential for successful absorption), this batch of capsules was "stickier" than previous batches. Hence the degree of fluidization was not complete.

The uptake curve for this run is shown in **Figure 69**, which was conducted at 73^{o}C and 0.007 bar CO_2.

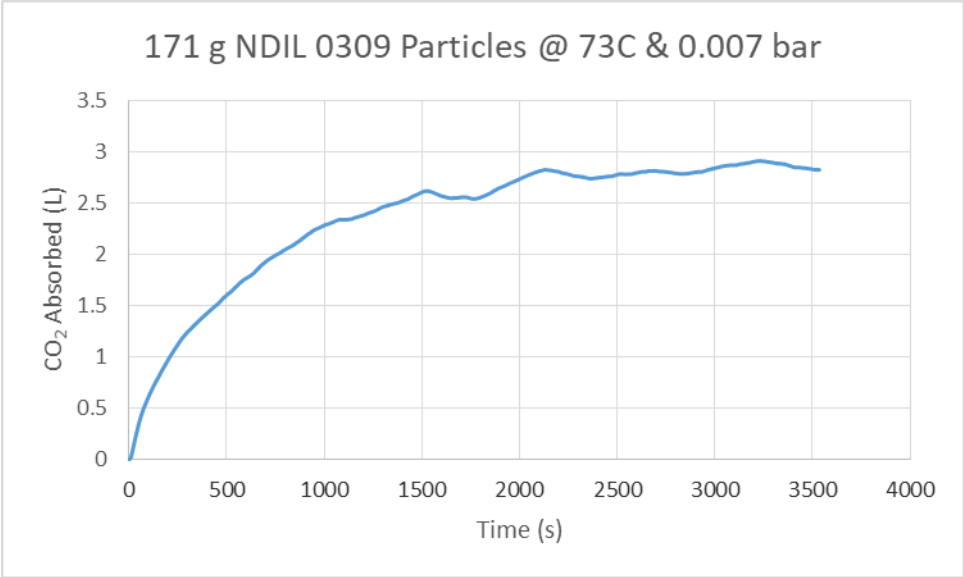

Figure 69: Fluidized bed CO_2 uptake (absorption) values vs. time for NDIL0309 - at 73°C and 0.007 bar CO_2

We see that this large quantity of capsules takes somewhat longer times to become saturated, which should make measurements of the mass transfer coefficients and total uptake more accurate.

We will continue to measure absorption/desorption rates with the new batches of capsules. We developed a procedure earlier this year for "de-clumping" and "de-sticking" the capsules.

Task 14.0 – Synthesis of additional small quantities of ILs for encapsulation for variable water permeability testing.

No work has been completed on this task to date. The Task and its associated Subtasks (14.1, 14.2, 14.3, 14.4, and 14.5) have been eliminated due to project redirection.

Task 15.0 – Encapsulation of ILs in shells with selectivity against water

Subtask 15.1 – Identification of hydrophobic membrane materials for selectivity against water with IL compatibility

The goal of this subtask is to decrease water vapor transport across capsule shell walls while maintaining high CO_2 permeability to (1) protect the ionic liquid core from chemical degradation and (2) reduce energy requirements of a capture system by eliminating the need to heat water during regeneration. Given the high CO_2 permeability and chemical compatibility of poly dimethyl siloxane (PDMS) based polymers for IL encapsulation, we chose to focus on modifying PDMS to reduce water vapor transport rather than selecting a different shell material.

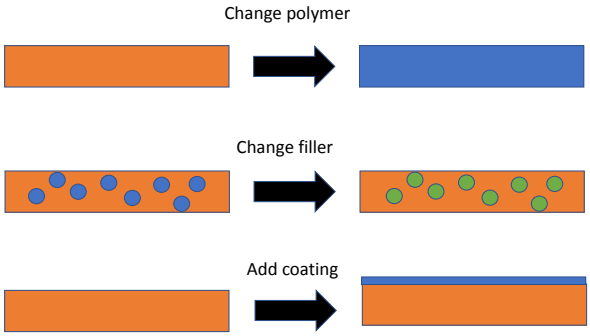

Figure 70: We explored reducing water vapor transport in PDMS by adding hydrophobic groups to the polymer backbone (top), increasing the hydrophobicity of the filler (middle) and adding a hydrophobic coating (bottom)

Additionally, a survey of the literature for PDMS alternatives did not reveal any candidate polymers with CO_2: water vapor selectivity that also had sufficiently high CO_2 permeability for our application (e.g. the best candidate is a Teflon based material, AF1600, has a CO_2: water vapor permeability ratio of 1:1, and a CO_2 permeability of about 500 barrer, coupled with poor processability). Unfortunately, while PDMS materials are chemically robust, easy to process, and CO_2 permeable, they selectively permeate water vapor vs. CO_2 with a ratio of 10:1. This is due to the small size of water molecules relative to CO_2 molecules, and the large free volume of silicones. Therefore, for this task we have focused on decreasing solubility of water in the shell materials by introducing perfluorinated and phenylated groups or hydrophobic fillers rather than attempting to decrease water vapor diffusivity. An illustration of the options that we explored are shown in **Figure 70**.

Given the established hydrophobicity of fluorinated polymers (e.g. Teflon), we first focused on synthesizing perfluorinated PDMS. The perfluorinated PDMS formulations were too brittle for practical use, and did not appear to reduce water vapor transport. Previously, we had promising qualitative results with phenylated PDMS. Therefore, we next explored the effects of phenylated PDMS more systematically by preparing formulations with varying mol % phenyl groups to identify whether mole % phenyl directly impacted water transport. The candidate samples were tested by replacing the septa in septum-sealed vials with the membranes of the candidate materials. We then added water to the vials, which were sealed with heat-resistant epoxy, placed the vials in an oven at 55 °C, and recording the mass change over time as water vapor permeated through the sample membranes.

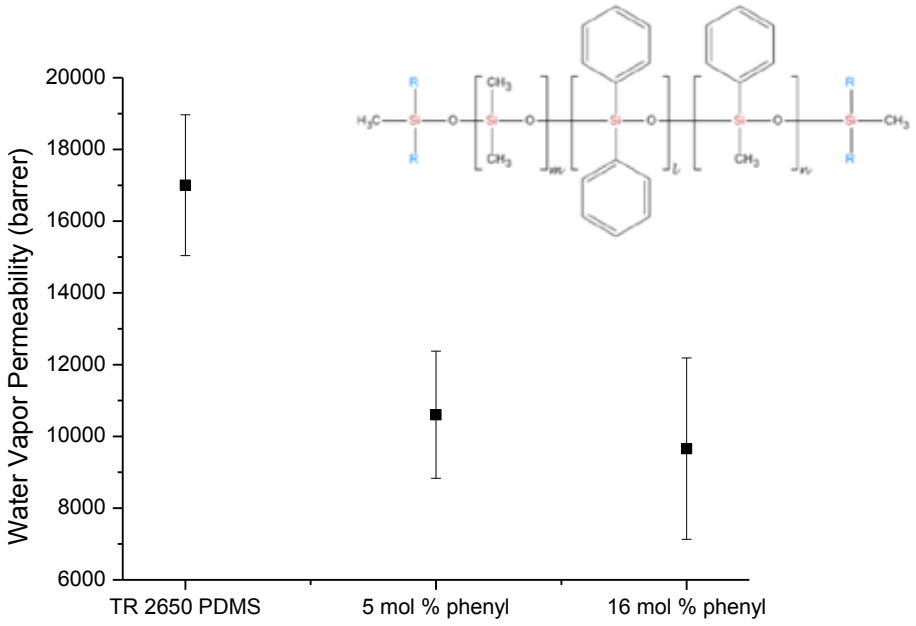

Figure 71. Water vapor permeability (n=2) of PDMS with varying mol% phenyl content. Inset: chemical structure of phenylated PDMS.

As shown in **Figure 71**, the relationship between phenyl content and water vapor permeability does not appear to be direct/linear, but verifying our initial preliminary results, we successfully reduced water vapor permeability of silicones by introducing phenyl groups to the silicone backbone. Unfortunately, we found that these phenylated membranes also had correspondingly lower CO_2 permeability (~1200 barrer at room temperature) than conventional PDMS, likely due to lower chain flexibility and lower free volume. The selectivity of the material for CO_2 over water was thus similar to conventional PDMS.

We subsequently turned toward modifying the fillers in PDMS rather than the chemistry of the polymer backbone to increase the hydrophobicity of the bulk material while maintaining CO_2 permeability. Fillers are typically inorganic silica based particles and are necessary to increase the mechanical strength of PDMS for practical use. Additionally, to increase the accuracy, throughput and reproducibility of our experiments, we designed and built custom water vapor permeation cells shown in **Figure 72**.

We compared water vapor transport between phenylated PDMS with our Thiolene-Q shell material loaded with a series of fluorinated and phenylated fillers. These fillers include fluorinated solid silica particles (shown schematically in **Figure 73**), phenylated porous silica particles (TEM image in **Figure 74**,) and fluorinated MQ-resin (synthesis shown in **Figure 75**). MQ resin is already used in our Thiolene-Q shell formulation for IL encapsulation to increase mechanical strength. Finally, a thin hydrophobic layer was added to the surface of our standard Thiolene-Q shell material using the commercial product Rain-X.

Figure 72: Custom cups for measuring mass loss of water across PDMS membranes.

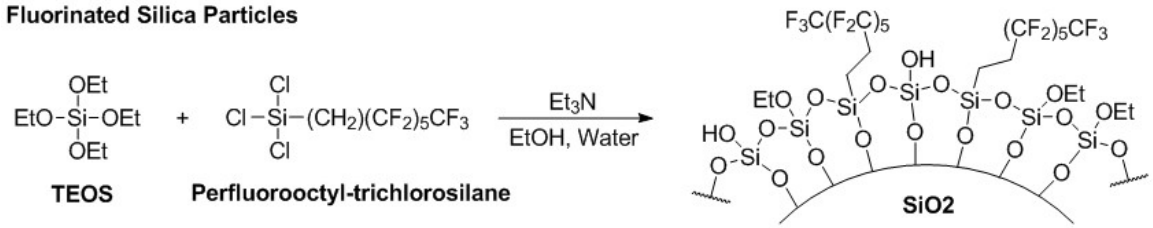

Figure 73.: Silica particle filler functionalized with perfluorinated groups.

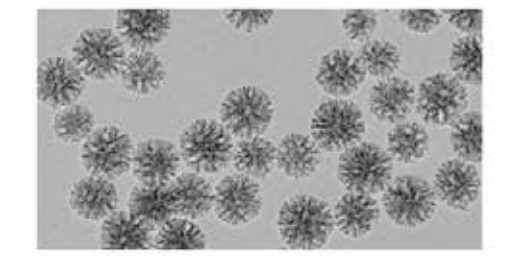

Figure 74: Porous silica fillers purchased from ACS chemical, image from ACS chemical. Silica was functionalized with phenyl groups prior to loading in PDMS. Our hypothesis was that the PDMS would bind to the mesopores of the silica, creating more selective, hydrophobic, glassy polymer regions that would prevent water vapor transport while allowing CO_2 transport through the pores.

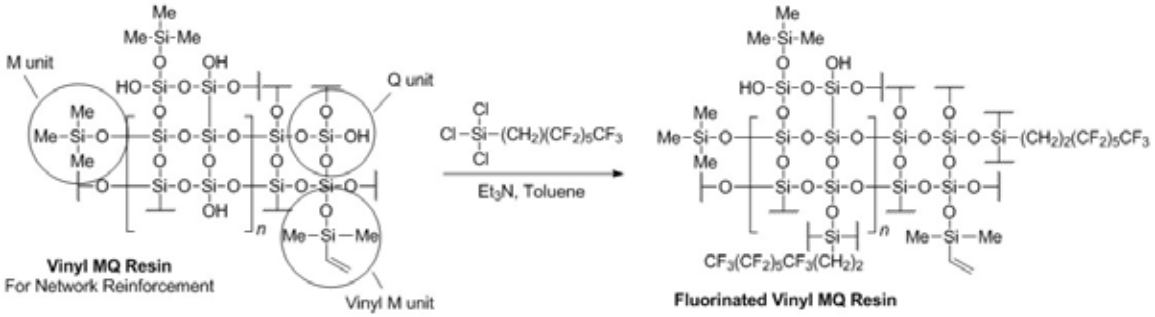

Figure 75: Procedure for modifying MQ resin with perfluorinated groups.

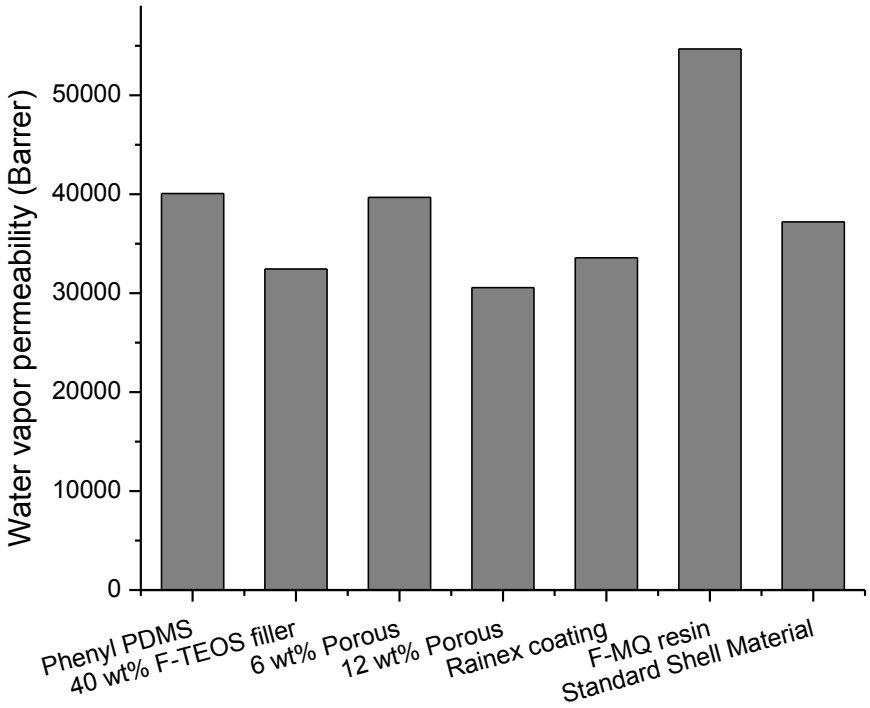

Figure 76: Comparison of water vapor permeability in various candidate shell materials

A comparison of water vapor permeability in phenylated, modified filler, and Rainex coated PDMS are shown in **Figure 76**. Whereas previous results indicated that the phenyl PDMS, fluorinated silica particles, and phenylated porous particles were promising (up to a twofold reduction in water vapor transport), the current data indicates comparatively less change in permeability. Since the previous tests were conducted at higher temperatures, it is possible that the selectivity is temperature dependent. Alternatively, since both silica fillers and PDMS hydrolyze in air over time, the filler surface chemistry and/or polymer chemistry may have changed. Ultimately, given the

fact that even our most promising candidates reduced water vapor transport by only a factor of 2, (a factor of 10 is desired), and the ILs were shown in Task 4 to be stable to water vapor, we determined that the development of hydrophobic capsules was not necessary to the successful completion of the project. Therefore, any further work on this subtask was suspended due to project redirection.

Subtask 15.2 – First production of small quantities (~25 g) of encapsulated ILs with water-selective shells

This subtask was eliminated due to project redirection.

Subtask 15.3 – Production of a suite of small quantities of encapsulated ILs with water-selective shells

This subtask was eliminated due to project redirection.

Task 16.0 – Testing of encapsulated ILs in water-selective shells

This task was eliminated due to project redirection.

CONCLUSIONS

IL NDIL0230 and PCIL NDIL0309 have been selected for encapsulation and demonstration in the laboratory scale CO_2 absorption/desorption unit. Small quantities of the IL and PCIL have been encapsulated in PDMS shells (called Thiolene-Q) and tested. When the samples do not contain broken shells, the CO_2 uptake matches that expected based on the content of the active material. The CO_2 uptake by the encapsulated NDIL0230 and NDIL0309 is reversible and recyclable. The IL and the PCIL, as well as their encapsulated versions, react irreversibly with NO_x and SO_2 so the CO_2 capture unit will need to be after the flue gas desulfurization and NO_x reduction units. On the other hand, the reaction of the IL and PCIL with CO_2 in the presence of water is completely reversible and the capsules can be cycled repeated. This discovery means that it is not necessary to develop water resistant shell materials and this is the basis of the redirection of the project away from these efforts. Scale-up methods have been identified for both the encapsulated NDIL0309 and NDIL0230. Kilogram quantities of the IL and PCIL have been synthesized and a cumulative quantity of about a kilogram of encapsulated NDIL0309 has been produced. The laboratory scale unit has been constructed and tested. I has been used to measure mass transfer rates, test fluidization, and measure absorption and desorption. Overall, the project appears to be on track to successfully demonstrate the benefits of encapsulating ILs and PCILs for post-combustion CO_2 capture.

ACKNOWLEDGEMENT

This material is based upon work supported by the Department of Energy under Award Number DE-FE0026465.